# OPTIMIZATION OF BIODIESEL PRODUCTION FROM ORANGE PEEL USING LIMESTONE BASED CALCIUM OXIDE CATALYST VIA IN SITU TRANSESTERIFICATION

**BY**

**YENKWO, Kwalna'an Catherine**
**(MEng/SEET/2017/6832)**

**A THESIS SUBMITTED TO THE POSTGRADUATE SCHOOL**
**FEDERAL UNIVERSITY OF TECHNOLOGY, MINNA, NIGERIA**
**IN PARTIAL FULFILMENT OF THE REQUIREMENTS FOR THE AWARD**
**OF THE DEGREE OF MASTERS OF ENGINEERING (MEng)**
**IN CHEMICAL ENGINEERING**

**JANUARY, 2022**

## ABSTRACT

The rise in population has led to high demand and consumption of petrol-based products thereby causing environmental concerns. In order to reduce the dependency on petrol-diesel, biodiesel has been found to be a suitable alternative. This study was carried out in order to determine the optimum conditions for biodiesel production from orange peel using limestone-based calcium oxide catalyst via in situ transesterification. Pre-treatment and characterization of orange peel was done. X-ray fluorescence (XRF) spectrometry of the limestone sample showed that it contained 55.04% of calcium oxide (CaO). The Fourier Transform-Infra Red (FTIR) analysis of the CaO catalyst revealed the absorption peaks at 3641.6 $cm^{-1}$, 1394 $cm^{-1}$, 872.2 $cm^{-1}$, and 711.9 $cm^{-1}$. The specific gravity and the kinematic viscosity of the biodiesel produced was 0.7580 and 0.8 $mm^2/s$ respectively. The optimization study was carried out using Design expert version 7.0 for the in situ transesterification experiment. The process parameters considered for the optimization study of the transesterification reaction resulted in an optimum Biodiesel yield of 70.10 % at methanol to oil ratio of 16.5:1, catalyst loading of 2.75 wt.%, reaction temperature and time of 85 $^oC$ and 100 minutes respectively. The $R^2$ for the in situ transesterification reaction was estimated to be 0.7015. Quality of biodiesel was successfully produced and it conformed to American Standards and Testing Materials (ASTM D6751).

.

## TABLE OF CONTENTS

## LIST OF TABLES

## LIST OF FIGURES

## LIST OF PLATES

ABU: Ahmadu Bello University.

**LIST OF PLATES**

ASTM: American Standard and Testing Materials.CaO: Calcium Oxide.

CCD: Central Composite Design.FAAE: Fatty acid alkyl esters.

FAME: Fatty acid methyl esters.FFA: Free fatty acid.

FUT: Federal University of Technology.GHG: Greenhouse gases.

IPCC: Intergovernmental Panel on Climate Change.JCB: Jathropha crude biodiesel.

JCO: Jathropha crude oil.

RSM: Response Surface Methodology.

USDA: United States Department of Agriculture.

# CHAPTER ONE

## 1.0 INTRODUCTION

### 1.1 Background to the Study

Fossil fuels, which are non-renewable, are formed from the geological transformation of buried organic materials over millions of years (Satyanarayana *et al*., 2011). The three examples of fossil fuels which are also the primary sources of global energy are petroleum, coal and natural gas (Dale, 2008; Yusuf *et al*., 2011). The rise in population has led to urbanization and demand for a better living standard, which has rapidly increased the demand and consumption of fossil fuel, particularly in the transportation sector, housing and industrial sectors (Sharma and Singh, 2009). The world is now facing the worst energy crisis due to the depletion of fossil fuel, fluctuation in oil prices, and increase in environmental concern due to emission of greenhouse gases (GHG) (Vlontzos and Pardalos, 2017).

According to the Intergovernmental Panel on Climate Change (IPCC), fossil fuel consumption contributes the largest to global anthropogenic greenhouse gas emissions (IPCC, 2012). The earth is estimated to be already warmed to about 1 $^{o}$C since pre-industrial times and is probably to continue warming above 2 °C increase except the concentration of GHG in the atmosphere becomes stabilize to about 500 ± 50 parts per million (Davis *et al*., 2011). This is the proposed range above which more harmful impacts of climate change such as rise in sea level, acidification of the oceans, drought and severe weather events are expected to worsen significantly (Robert, 2013).

These factors have caused worldwide concerns and have resulted in the search for alternative source of energy which would be renewable and sustainable. One method of reducing the rise in energy-related emission of GHG is to substitute the conventional

fossil fuels with biofuel, which include energy derived from biomass. The advantages of using biofuel can be summarized in three aspects: environment, energy security, and economy (Demirbas, 2009). It is assumed that carbon released during the combustion of such biofuels is biogenic and therefore does not increase the overall concentration of GHG in the atmosphere (Robert, 2013); also, biofuels are biodegradable, less toxic, and can be converted from common and abundant biomass sources which contribute to sustainability and the reduction of fossil fuel consumption. For the aspect of economy, the development and use of biofuel will help to create jobs related to biofuel generating industry (Narasimharao, *et al*., 2007).

Biofuels are produced from edible and non-edible natural materials such as agricultural and forestry by-products, grain and oil crops, used cooking fats or waste oils, animal fats and seeds. Biofuels can be solid (bio-coal), liquid (bioethanol, vegetable oil, and biodiesel), or gaseous (biogas, biosyngas, and biohydrogen) fuel that is produced predominantly from biomass (Demirbas, 2010). According to the United States Department of Agriculture (USDA), the two most widely used liquid biofuels presently are bioethanol, derived from fermenting sugarcane and corn, and biodiesel, produced by transesterifying vegetable oils from soybean, rapeseed, palm, and other similar oil seeds (USDA, 2013). Liquid biofuels, such as biodiesel and bioethanol, can offer a promising alternative to petroleum fuel because of their comparable properties: they can be directly used as fuel, although they may require some engine modifications, or blended with petroleum diesel and used in diesel engines with little or no modifications (Taiichiro and Shigenori, 2010). Biodiesel is non-toxic, biodegradable, produced from renewable sources and contributes a negligible amount of net greenhouse gases, such as $CO_2$ and $NO_2$ (Tasyurek *et al*., 2010). Thus, biodiesel may be considered as a very good and favourable alternative source of energy (Taiichiro and Shigenori, 2010).

Regardless of these advantages, some factors are still not favourable for the production of biodiesel. The use of edible oil to produce biodiesel is not feasible because of the big gap in demand and supply of such oils in the country for food consumption. The increase in pressure to boost the production of edible oils has also put limitations on the use of these oils for production of biodiesel (Sinha *et al*., 2008). Biodiesel is therefore, actually competing for the limited land available with the food industry for the same oil crop. This will then increase the price of edible oil making the biodiesel produced not to be economical as compared to petroleum-derived diesel. In order to overcome this issue, many researchers have started searching for cheaper, non-edible and abundant oils to be used as alternative feedstock for biodiesel production (Kansedo *et al*., 2009). Few sources have been identified such as waste cooking oil (Chen *et al*., 2009) and oils from non-edible oil-producing plants such as jatropha curcas and rubber seeds (Ramadhas *et al*., 2005) and tobacco seeds (Usta, 2005) and neem seed (Tiwari *et al*., 2007). However, there is little information in the literature on the use of oils obtained from discarded orange peels.

On account of the recent food crisis that resulted from food materials being converted to biofuels, the need to consider waste peels of orange fruits as source of potential oil for biodiesel production cannot be over emphasized (Agarry *et al*., 2013). Nigeria has an enormous potential for producing more oranges and the orange peels are a direct source of environmental degradation with reference to the dumping thereof in landfills. In Nigeria, about 930,000 tons of citrus fruits are produced annually from an estimate of 3,000,000 hectares (Njoku and Evbuomwan, 2014); Nigeria also has the potential for producing between 233,859 to 485,554 litres of orange peel oil per annum based on 0.2% recovery-rate of orange-peel oil by the cold-press process considering a 70% harvest

viability of 1,626,000 tons of sweet orange fruits (Njoku and Evbuomwan, 2014). In 2018, the annual world production of oranges was estimated to be 4,930,000 tons (USDA, 2018). Nigeria is ranked ninth in the world amongst the leading citrus producing countries and first in Africa, producing 3,330,000 tons of citrus fruits (The Daily Records, 2018). Looking at the prospective benefits of tapping into this rich source of biofuel by producing orange oil for use in diesel engines, it has therefore become important to assess the production potentials of orange oil in Nigeria for use in diesel engines (Akpan *et al*., 2014).

There are several methods for the production and application of biodiesel such as direct use of vegetable oils, micro emulsions, thermal cracking (pyrolysis) and transesterification. Transesterification is widely used for its advantages such as renewability, higher cetane number, lower emissions and higher combustion efficiency (Leung *et al*., 2010). It is the reaction of triglycerides with an alcohol in the presence of a suitable catalyst to produce a mixture of fatty acid alkyl esters (FAAE) and glycerol (Poonam and Anoop, 2010). The stoichiometric reaction requires 1 mole of triglycerides and 3 moles of alcohol; it consists of three reversible steps of reaction. However, excess alcohol is required to drive the reaction close to completion (Borges and Diaz, 2012). In recent years, researchers studied extensively to improve the transesterification process by the variation of the reaction conditions like the choice of catalyst, oil/alcohol ratio, temperature and reaction time (Bradley *et al*., 2011; Veillette *et al*., 2017). An improved upon method of transesterification is the in situ transesterification which does not involve extraction of oil from feedstock. It would therefore, be less stressful and cheaper to extract and convert the triglycerides from the orange peel oil into biodiesel in a single step, avoiding the use of large amounts of organic solvents (Chattip *et al*., 2012). The advantage of this integrated stage includes lower production cost of biodiesel production

by reduction of reagents and solvents. Also, the concern on waste disposal can be avoided (Abo *et al*., 2013). The in situ transesterification methods have been evaluated for biodiesel production from various raw materials, such as vegetable oil (Haas and Scott, 2007), rice bran oil (Shiu *et al*., 2010), cotton seed oil (Leung *et al*., 2010), microalgae (Li *et al*., 2011) and orange peel (Yahaya *et al*., 2014). It was reported that the in situ method may produce higher yields of FAAE than those obtained from the conventional transesterification (Bradley *et al*., 2011). The in situ transesterification process, like conventional reaction, uses acid, basic or enzymatic catalysts. Heterogeneous catalysts are another alternative for the production of biodiesel. Heterogeneous catalysts can be easily separated from the biodiesel by filtration and they may be recycled. In addition, heterogeneous catalyst may eliminate the need for water washing of biodiesel, as the catalyst is not dissolved in the biodiesel.

In general, heterogeneous base catalysts are more active and less corrosive than the heterogeneous acid catalysts and are more favoured for biodiesel transesterification reaction. Base heterogeneous catalysts that have been studied include mixed oxide of zinc and aluminium, calcium methoxide, alumina-supported potassium iodide, and calcium oxide. Among heterogeneous base catalysts, calcium oxide (CaO) is the most studied and widely used as it presents many advantages such as longer catalyst life, high activity and requires only moderate reaction conditions (Aqliliriana *et al*., 2015).

There are quite a number of researches that have been carried out on transesterification of orange peel oil; however, this research aims to optimize the production of biodiesel from orange peel using limestone-based calcium oxide catalyst via in situ transesterification in the presence of methanol as solvent.

## 1.2 Statement of the Research Problem

As population continues to rise, worldwide energy demand, particularly for high-density liquid transportation fuels increases. Just as fossil fuel consumption today contributes to climate change, ecosystem damage, and poor energy security for many nations, meeting future demands for energy by using more fossil fuels will only continue to intensify these consequences. Most traditional sources of biofuels are classic agricultural food crops that require high-quality agricultural land for growth; biodiesel is therefore, actually competing with the limited land available with the food industry for the same oil crop (Sinha *et al*., 2008). The conventional method for producing biodiesel involves the extraction of oil and transesterification of the oil, generally in the production of biodiesel, homogeneous base or acid is used as catalyst (Leung *et al*., 2010). However, the process of separating the catalyst from biodiesel is quite difficult, requires washing with water which results in loss of fatty acid methyl esters (FAME), energy consumption, and generates large amounts of waste water.

## 1.3 Justification of the Study

Increase in population has led to increase in demand and consumption of petrol-diesel which in turn contributes to climate change, ecosystem damage, and poor energy security for many nations. Biodiesel, when compared to petrol-diesel, has improved fuel performance, higher cetane rating, a higher flashpoint that makes it safe to handle, lower toxicity to plants and animals, reduced exhaust emissions. It will therefore decrease the dependency and hence consumption of fossil fuel, reduce the emission of GHG and also improve energy security. Biodiesel produced from edible oil is not practical because of the big gap in demand and supply of such oils in the country for dietary consumption.

Most oranges produced in Nigeria are eaten locally, Nigeria still has a huge potential for producing more oranges and the orange peels are a direct source of environmental

degradation through the dumping that fills landfills. Looking at the potential benefits of tapping into this rich source of biofuel by producing orange peel for use in diesel engines, it has therefore become important to assess the production potentials of orange peel in Nigeria for use in diesel engines.

Methanol is used widely because it is relatively cheaper than other alcohols and has chemical and physical advantages over other alcohols (Leung *et al*., 2010). The economic advantage of using heterogeneous catalysts is the simplicity of their isolation from the reaction mixture to purify the viscous product, which makes the reaction a short time experience in comparison with similar processes (Vafakish and Barari, 2017). Calcium oxide (CaO) catalyst from limestone has been listed to be among the most promising catalyst because of its abundance in nature and also in Nigeria (Felix and Yomi, 2013).

### 1.4 Aim and Objectives of the Study

The aim of this research work is to use available non-edible feedstock (orange peel) to produce quality biodiesel through a cheap process (in situ transesterification).

The aim will be achieved through the following objectives;

i Synthesis of calcium oxide catalyst from limestone.

ii Characterization of the calcium oxide catalyst for morphology, size, and surface area.

iii Extraction of oil from orange peel for its characterization (only).

iv Production and characterization of biodiesel produced via in situ transesterification from orange peel.

V Optimization of biodiesel production via in situ transesterification from orange peel.

## 1.5 Scope of the Study

**LIST OF PLATES**

This research focused on the use of locally sourced orange peel within Jebbu Bassa in Plateau State and limestone from Obajana in Kogi State. Oil from orange peel was extracted through soxhlet for the sole purpose of characterization. Calcination of limestone obtained was done to synthesize calcium oxide catalyst which was used in in situ transesterification reaction of orange peel with methanol. This study also characterized the catalyst and biodiesel obtained by determining important parameters and optimizing the process.

# 2.0 LITERATURE REVIEW

## 2.1 Background to the Study

Man's desire to live comfortably has led to improvement in areas of his life such as food, shelter, clothing, energy, and transport. These factors have increased the demand in petroleum and petroleum products thereby causing increase in environmental concerns due to emission of GHG. This has steered government of nations and researchers alike towards energy diversification which is renewable, available and environmentally friendly. The production of biodiesel from available, cheap and environmentally friendly feedstock is presently one of the novel technologies towards energy independence in the world (Sharma and Singh, 2009). Optimization of production variables as regards to the maximization of quality, profitability, and safety is of utmost importance to researchers and stakeholders today. As such this chapter summarizes the historical background of biodiesel and review of work carried out by researchers in the field of production of biodiesel from different feedstock, biodiesel production techniques, biodiesel fuel properties, and controlling factors of biodiesel production, application of Central Composite Design (CCD) of Response Surface Methodology (RSM) as a relevant optimization tool for biodiesel production.

## 2.2 History of Biodiesel

Biodiesel is an environmentally friendly alternative liquid diesel fuel resulting from the transesterification of vegetable oil or animal oil with alcohol in the presence of a suitable catalyst (El-Shimi *et al*., 2013). Transesterification reaction was first conducted by Scientists E. Duffy and J. Patrick as far back as 1853 (Dokwadanyi, 2011). During the 1911 World's Fair in Paris, Rudolf operated his engine using peanut oil and declared 'the diesel engine can be fed with vegetable oils and will help considerably in the development

of the agriculture of the countries which is one of the first uses of transesterified vegetable oil was powering heavy-duty vehicles in South Africa before World War II (Dokwadanyi, 2011). Certain operative problems were reported caused by the high viscosity of vegetable oils compared to petroleum diesel fuel, which results in poor atomization of the fuel in the fuel spray which often results in deposits and coking of the injectors, combustion chamber and valves. Efforts to overcome these problems involved heating of the vegetable oil, blending it with petroleum-derived diesel fuel or ethanol, pyrolysis and cracking of the oils (Abdulkareem *et al*., 2011). By 1998, the Austrian Biofuels Institute had identified 21 countries with commercial biodiesel projects. In September 2005 Minnesota became the first U.S. State to decree that all diesel fuel sold in the state contain at least 2% biodiesel (Dokwadanyi, 2011). Biodiesel is the only alternative fuel that can be used directly in any existing unmodified diesel engine. Report has shown that biodiesel can be combined with the diesel fuel in any proportion due to the resemblances in their properties and the existing trends in the production of biodiesel from vegetable are now focused on non-edible oil as the feedstock (Abdulkareem *et al*., 2011).

## 2.3 Biodiesel

Biodiesel is a non-petroleum-based diesel fuel which comprises of long chain fatty acid of mono alkyl esters gotten from renewable lipid sources. It is an environmentally friendly fuel that can be used in any diesel engine without modification (Atabani *et al*., 2012)**.** In simple terms, biodiesel is produced when vegetable oil or animal fat reacts chemically with alcohol to produce fatty acid alkyl esters in the presence of a catalyst (Abdulkareem *et al*., 2011). It is made up of $C_{14}$–$C_{24}$ carbon chains and can be represented chemically as $C_{15\text{-}25}\ H_{28\text{-}48}\ O_2$ (Ngoya, 2015). Biodiesel is made up of five main saturated and unsaturated methyl esters, depending on the type of oil used namely; methyl palmitate -

$C_{17}H_{34}O_2$, methyl stearate - $C_{19}H_{36}O_2$, methyl oleate - $C_{19}H_{34}O_2$, methyl linoleate and methyl linolenate - $C_{19}H_{30}O_2$ (Grana *et al*., 2012). Biodiesel offers several advantages as an alternative fuel for diesel engines, these include improved fuel performance and lubricity, a higher cetane rating, a higher flashpoint which makes it safe to handle, lower toxicity to plants and animals, lower exhaust emissions and the fact that it is simple to phase in and out of use (Sivaramakrishnan and Ravikumar, 2012). It is a local renewable source of energy and highly biodegradable (Meo *et al*., 2017).

## 2.4 Biodiesel Production Techniques

A number of methods can be used for the production and application of biodiesel which include direct use of vegetable oil, microemulsions, thermal cracking (pyrolysis), and transesterification (Casas *et al*., 2015). Direct use of vegetable oil had several problems such as coking of injector, thickening of lubricants, and oil deposits were recorded on extended operation of diesel engine (Gupta *et al*., 2007). These problems occur because of vegetable oil has higher viscosity, reduced volatility and the reactivity of unsaturated hydrocarbon chains (Farizul *et al*., 2010). Microemulsions effectively reduced the viscosity of vegetable oil, carbon deposits were however increase on the injector tips, intake valve and tops of cylinder liners (Satyanarayana and Muraleedharan, 2010). Thermal cracking (pyrolysis) and transesterification were introduced in the pre-1990s. The production of biodiesel by transesterification process usually uses pre-extracted oil as raw material, which is usually produced by mechanical pressing followed by solvent extraction to extract the remaining oil, and then its conversion to biodiesel and glycerol (El-Shimi *et al*., 2013). Not only was the quality of biodiesel produced through this technology similar to that of petroleum diesel, but the process could also be operated at low temperature (typically 60 $^{o}$C) and low pressure, resulting in relatively low energy consumption. Furthermore, the fuel performed well in engine tests (Satyanarayana and

Muraleedharan, 2010). However, it was also discovered that ester yields were reduced due to the existence of gums and extraneous material in the crude vegetable oil hence research into in situ transesterification was also reported at this time, particularly by Harrington and D'Arcy-Evans (Farizul *et al*., 2010). In situ transesterification combines the oil extraction and esterification/transesterification and direct contact between the oil with alcohol, such that the alcohol plays a dual role of an extraction solvent and transesterification reagent (Widayat *et al*., 2017).

### 2.4.1 In situ transesterification

The production of biodiesel is usually by transesterification of vegetable oils using alcohol in the presence of a catalyst. This process often uses pre-extracted oil as the raw material, which is usually produced by pressing the oil-bearing seeds, then followed by solvent extraction to extract any remaining oil (Farizul *et al*., 2010). On the other hand, the production of biodiesel can be done via in situ transesterification or reactive extraction. In this process oil-bearing seeds are soaked, then directly reacted with the alcohol and catalyst, by this means removing the need for pre-extracted oil, and its associated capital and running cost intensive production methods. A comparison of both methods is captured in Figure 2.1. Bradley *et al*. (2011) reported that the in situ transesterification process may result in higher yields of FAME than those obtained from the conventional method.

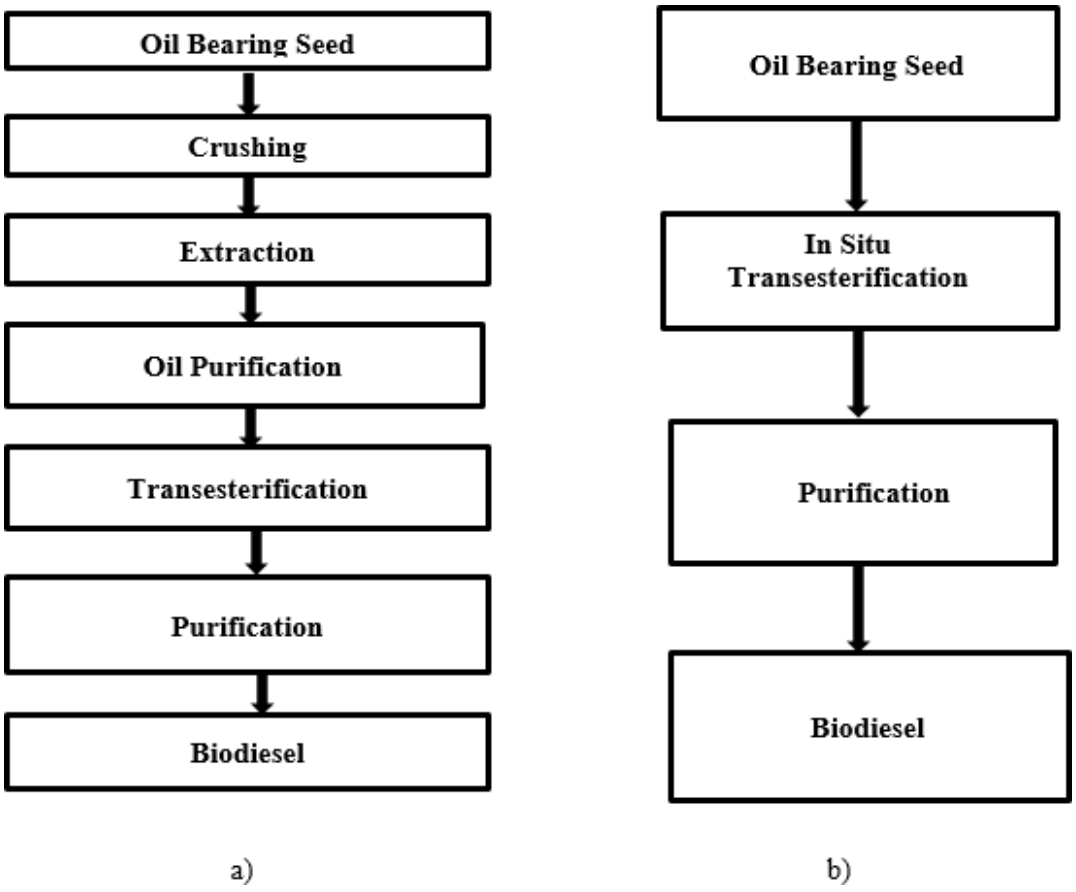


**Figure 2.1:** The scheme of biodiesel production by use of a) conventional and b) in situ transesterification method (Sevil and Pinar, 2013).

According to Farizul *et al*. (2010), Harrington and D'Arcy first compared the process of in situ transesterification and the conventional transesterification using sunflower seed as feedstock in 1985, they achieved up to 20% increase in yield of biodiesel production in the in situ transesterification as compared to the conventional method. Sanjaykumar *et al.* (2012) concluded that biodiesel can be produced directly from undi seeds via in situ transesterification process with the optimum concentration of potassium hydroxide, methanol and ethanol. Their work showed that the biodiesel fraction from oil content was 74.5% at 60 ºC and 400 rpm oscillations for 60 minutes and normal atmospheric pressure without addition of water in the reaction mixture. Ika *et al.* (2016) successfully carried out in situ transesterification of jathropha seeds and obtained a yield of 92% and a FAME purity of more than 98%. Marian and Ihab (2014) compared in situ transesterification

process and the conventional method of biodiesel production using *Chlorella vulgaris*. Their result showed that the in situ biodiesel produced a higher FAME yield (55.52 g FAME/g dry *Chlorella vulgaris* algae) than the two-step process (4.03 g FAME /g dry *Chlorella vulgaris* algae). They added that the in situ process takes less time in the lab and does not use hazardous and expensive n-hexane solvent.

Factors like catalyst type, molar ratio of alcohol to oil, reaction temperature, catalyst concentration, alcohol type, and agitation intensity play important roles in determining the conversion, reaction rate, and quality of the biodiesel in in situ transesterification (Farizul *et al*., 2010). Ryan *et al.* (2013) investigated the in situ transesterification of jatropha seed for biodiesel production. Their experimental results showed that the moisture content of jatropha seeds and the amount of co solvent of hexane, and interaction both have very significant effect on the yield of biodiesel produced. Their result showed that the highest biodiesel yield of 74.56% was obtained on experimental condition of moisture content of 2% and hexane amount of 95 mL. Ehimen *et al.* (2012) investigated the influence of reacting alcohol volumes, temperature, reaction time, biomass moisture content and stirring in in situ transesterification of microalgae lipids, their results showed that production of biodiesel is favoured by increase in alcohol volume and reaction temperature. Considerable improvement in biodiesel yields were observed with process stirring. They suggested that some savings may be achieved in the stirring energy since the reactors can be stirred occasionally without a significant drop in the yield. They also observed that biomass drying played an important role, decrease in the moisture content of the biomass resulting in substantial increase of the equilibrium FAME conversion yields.

## 2.5 Feedstock for Biodiesel Production

LIST OF PLATES

Due to their nontoxicity, biodegradability, inexhaustibility, benignity, and renewability, vegetative plant oils are considered the most suitable and efficient raw material for the production of biodiesel. However, based on regional environmental circumstances, socioeconomic apprehensions and government strategies, availability of plant oil differs significantly in different countries (Patrick *et al*., 2013). There are two categories of feedstock for biodiesel production namely the liquid feedstock and alcoholic feedstock (Tshizanga, *et al*., 2017). Liquid feedstocks are classified into three generations (Nagarajan *et al*., 2012). First generation liquid biofuels are feedstock with very low free fatty acid (FFA) that needs no pre-treatment before use for biodiesel production; they are produced from food crops such as corn, sugarcane and vegetable oils.

The production of first-generation liquid biofuels was at a great disadvantage because the feedstocks used were food crops, it was affected by food supply and increasing the food prices. This paved the way for second generation liquid biofuels, which contains high amount of FFA (2% to 50%), not suitable for human consumption, not expensive but require pre-treatment before use for biodiesel production. The feedstocks used were waste vegetable oil; waste cooking oil, non-edible plant seed oil, and animal fats (Nagarajan *et al*., 2012). Even though second-generation liquid biofuels overcame the problems faced by the first-generation liquid biofuels, difficulties like increase in the consumption of fuel and challenge for the constant supply with consistent feedstock led to the development of third generation liquid biofuels like algae biodiesel, they contain high amount of FFA (2% to 40%) depending on initial usage and may require pre-treatment before usage for biodiesel production (Jones and Mayfieldt, 2012). Alcoholic feedstock comprises of chemical compounds that contains alcoholic ring like methanol, ethanol, isopropanol,

butanol among others. Various liquid feedstock for biodiesel production is shown in Table 2.1.



**Table 2.1:** Various Liquid Feedstock for Biodiesel Production (Atabani *et al*., 2012)

| Edible oil | Non edible oil | Animal fat | Other sources |
|---|---|---|---|
| Corn oil | Mahua oil | Pork | Algae oil |
| Coconut oil | Jatropha oil | Lard | Bacterial |
| Canola oil | Neem oil | Beef tallow | Latexes |
| Peanut oil | Cotton seed oil | Poultry fat | |
| Palm oil | Jojoba oil | Chicken fat | |
| Tobacco seed oil | Switch grass oil | Fish oil | |
| Moringa seed oil | Camelina oil | | |
| Coconut oil | Karanja oil | | |
| Castor seed oil | Pongamia seed oil | | |
| Bailey oil | Cumaru oil | | |
| Safflower oil | Salmon oil | | |
| Rice bran oil | | | |

Selection of feedstock for the production of biodiesel is very important because the cost of raw materials accounts for about 60% to 80% of the total cost of the production (Leung *et al*., 2010).

### 2.5.1 Orange peel

Tobias *et al.* (2011) reported that the total production of oranges in Nigeria has fallen to approximately 300,000 tons of oranges annually. This fall in production level records may be ascribed to security challenges which can affect the farmers and even the officials who are supposed to capture the data. Despite these challenges, Nigeria still has a vast prospective for generating more oranges and therefore, orange wastes (orange peels and orange seeds). Due to the current food crisis that is asserted to be as a result of conversion of food materials to biofuels, the need to consider waste of citrus fruits as source of potential oil for biodiesel production cannot be over stressed (Agarry *et al*., 2013). Looking at the possible benefits of tapping into this rich source, it is therefore important to evaluate the production potential of orange peel as feedstock for biodiesel production (Akpan *et al*., 2014). A number of research has been done on biodiesel production from citrus seed waste, particularly orange.

Bull and Obunwo, (2014) investigated the production of biodiesel from orange peel, their findings suggested that the condition of orange peels oil biodiesel produced were 1:3 oil to ethanol volumetric ratio, 1 g NaOH at 80 $^{o}$C to 83 $^{o}$C reaction temperature. Their study confirmed that oil from orange peels could be used as a significant feedstock for the production of biodiesel, because the quality of the biodiesel produced was within the American Standards and Testing Materials (ASTM) standard method specification. Anusi *et al*. (2018) characterized the oil obtained from orange peels and velvet tamarind nut for biodiesel production to determine some of the suitable parameters such as iodine value, saponification value, specific gravity, density, acid value and free fatty acid value, and their percentage yield that are suitable for biodiesel production. The various values obtained were compared with specifications of ASTM D6751 and was clearly confirmed that the properties of both orange oil and velvet tamarind oil have shown to be suitable feedstock for high quality biodiesel production.

### 2.5.2 Alcohol

Alcohol is one of the most important liquid feedstock required for the production of biodiesel (Tshizanga *et al*., 2017). In in situ transesterification, alcohol acts as both an extraction solvent and an esterification reagent, which could reduce the production time associated with pre-extracting the oil and maximize the fatty acid ester yield (Ga *et al*., 2014). Methanol is the most frequently used alcohol compared to other types of alcohol such as ethanol and butanol because it reacts the most rapidly, it is readily obtainable and reasonably cheap. It is of economic benefit, has low viscosity, lower molecular weight (32.04 g/mol), require less reaction time and has high performance (Tshizanga *et al*., 2017). Tsigie *et al.* (2012) investigated the influence of methanol on the amount of FAME content in the in situ transesterification of wet *Chlorella vulgaris* biomass at 175 °C and after 4 h under subcritical condition. They observed that a 1:4 (w/w) ratio of a wet

microalgae biomass to methanol was the optimal ratio and additional increase in methanol amount reduced the conversion of crude microalgal oil to biodiesel. Abo *et al*. (2013) investigated the alkali-catalysed in situ transesterification of rapeseed in order to detect the effect of changes in molar ratio of methanol to oil in seeds on the yield. The experiments were carried out with the molar ratio of methanol to oil within the range of 360 to 1440. At a methanol to oil molar ratio of close to 720:1, the yield was 90%. In spite of the yield being higher (96%) at 1440:1 ratio, the ratio of 720:1 was preferred as an optimum due to economic reasons.

### 2.5.3 Catalyst

A catalyst is a substance that speeds up or reduces the speed at which a reaction takes place. Researchers have observed that the choice of catalyst for biodiesel production depends on a number of factors like type of feedstock (edible or inedible), exposed surface area, thermal stability, conversion rate, deactivation, operating conditions (temperature, pressure and concentration), cost and availability (Tshizanga *et al*., 2017). As a result, it was suggested that a good catalyst for biodiesel production must have high surface area, be thermally stable, have low deactivation rate, activated at low temperature and have high selectivity (Refaat, 2010). Therefore, researchers have increased their interest in developing catalysts which will efficiently develop the quality and also decrease the general price of biodiesel produced. The in situ transesterification process, like conventional reaction, uses acid, basic or enzymatic catalysts. The use of catalyst is characteristically affected by the FFA content of the feedstock. Alkaline catalysts are used when the FFA content of the feedstock is <0.5% w/w (based on oil weight), this is because the use of alkaline catalysts with oils that contain high FFA would lead to a partial saponification reaction, leading to the soap formation and difficulties in the biodiesel separation and purification downstream. Typically, there are two kinds of catalysts which

are used in any biodiesel production process: the homogeneous and heterogeneous catalysts. Homogeneous catalysts which function in the same phase as the reactants, they usually dissolve in a solvent with the substrates (Amrik and Kumar, 2018). However, there are some concerns associated with conventional homogenous catalysts such as higher acid number, yield loss, higher post cleaning cost, their sensitivity to FFAs and water, corrosive nature, their reusability and the resulting saponification phenomenon. Furthermore, the formation of immiscible glycerol phase in the course of the process of the reaction solubilizes the homogeneous base catalyst and, therefore, withdraws it from the reaction (Amrik and Kumar, 2018).

Heterogeneous catalysts occur in a different phase from the reactants. The total surface area of the heterogeneous catalyst has a significant effect on the reaction rate; the smaller the catalyst particle size, the larger the surface area for a given mass of particles (Idris, 2016). The surface of heterogeneous catalyst must be hydrophobic in nature so that it adsorbs triglyceride and to avoid adsorption of polar by products like water and glycerol on surface (Amrik and Kumar, 2018). Base-catalysed in situ transesterification can be carried out using base homogeneous catalyst and a heterogeneous catalyst such as KOH, NaOH, and CaO (Ummu *et al*., 2018). The process of biodiesel production has been recognised and commercialized using homogeneous catalysts; however, homogeneous catalysts are difficult to separate from the product mixture. Hence, a large amount of polluted water was created to get rid of the basic catalyst from the biodiesel product (Idris, 2016). Several researchers embarked on exploration of the activities of wide range of heterogeneous catalysts in a massive attempt to reduce the problems associated with homogeneous catalysts. Heterogeneous catalysts can be easily separated from the biodiesel by filtration. In addition, heterogeneous catalyst eliminates the need for water washing of biodiesel, as the catalyst is not dissolved in the biodiesel. The major problem

with heterogeneously catalysed biodiesel production is that it has a low reaction rate compared to homogeneous catalysis. To overcome this major challenge, the reaction conditions of heterogeneous catalysis are strengthened by increasing reaction temperature, catalyst amount and methanol/oil ratio (Boro *et al*., 2014). Hattori classified solid base heterogeneous catalysts into six categories namely - single metal oxide, mixed metal oxide, supported alkali, alkali earth metals, hydrotalcites and organic base solids (Iman *et al*., 2017). The most usually used for biodiesel production are the single metal oxides because their catalytic activity is directly related to the basicity of the oxide (Jacques, 2017). Examples of single metal oxide base catalyst used in biodiesel production are calcium oxide (CaO), magnesium oxide, zinc oxide, zirconia oxide, tin oxide and strontium oxide (Sharma *et al*., 2013). Among these single metal oxides, CaO has been chosen from economic and ecological point of view to be the most popular and promising single metal oxide catalyst for use in biodiesel synthesis due to its excellent catalytic activity, long catalyst life, active in moderate temperature, high basic strength, abundance in nature, lower price, ease of handling and environmental benignity (Yoosuk *et al*., 2010; Aqliliriana *et al*., 2015; Tshizanga *et al*., 2017).

Nur *et al*. (2016) studied in situ transesterification using solid coconut waste and a heterogeneous catalyst synthesized from eggshells and solid coconut waste by calcination. The reaction temperature ranges from 70 ˚C to 120 ˚C, catalyst loading was 0.5 to 10.5 wt%, methanol to solid ratio was varied from 8:1 to 12:1, and the reaction time was fixed at 3 hours. They concluded that heterogeneous catalyst helped to reduce the steps in separation and purification of the product. The highest biodiesel yield observed from their experimental conditions was temperature of 95˚C, 0.5 wt% catalyst, and 10:1 methanol to solid ratio. In situ transesterification of cottonseeds oil (*Gossypium Spp*) using CaO derived from egg shell as catalyst was investigated by Sani *et al*. (2018), 5 g

CaO derived from egg shell as catalyst using soxhlet extraction apparatus and 1:1 of n-hexane to methanol at a temperature of 60 $^{o}$C for 2 hours. The biodiesel yield was 35.75%, content of water and sediment was 0.08%, density was 0.85 g/cm$^3$, and specific gravity was 0.85. they concluded that the profile of the FAME was within the ASTM6571 standard approved specification for biodiesel to be used as fuel are all. Muhammad *et al*. (2018) carried out the in situ transesterification of *Datura metel* seed oil with 1:1 methanol to n-hexane co-solvent and CaO derived from snail shell as catalyst at a temperature 65 ℃ for 3 hours in soxhlet extraction apparatus. The prepared CaO from snail shell produce high biodiesel yield of 91% which indicates high CaO catalyst activity, the heating value was close to petro-diesel and cetane number higher than the minimum standard set by ASTM. The density of *Datura metel* seed oil biodiesel is within ASTM Specification but it records high acid value.

#### *2.5.3.1 Limestone as source of calcium oxide catalyst*

A new method for preparing CaO catalyst that is presently being studied for optimum production of biodiesel is the utilization of natural calcium sources from waste materials. Types of waste sources from which basic heterogeneous catalyst can be gotten are shells, ashes, rocks and clay bones (Nurfitri *et al*., 2013). It is a well-known fact that catalyst produced from natural sources has great potential for use in commercial biodiesel production because of their availability, abundance, low cost, high catalytic activity, and renewability. This development involves the use of calcination as a vital stage for the decomposition of different natural raw materials as source for calcite ($CaCO_3$) and formation of CaO (Zeljka *et al*., 2016).

Limestone is a sedimentary rock predominantly made up of mineral calcite ($CaCO_3$) formed either by organic or inorganic processes (Fatoye and Gideon, 2013). It contains

90 - 95% $CaCO_3$ and 10 - 5% of other mineral depending on its purity (Itodo *et al*., 2017). Nigeria has large deposit of limestone in 22 locations scattered across various sedimentary basins namely Niger Delta, the Benue Trough, the Chad Basin, the Sokoto Basin, the Mid-Niger (Nupe/Bida) Basin and the Dahomey Basin (Akinniyi and Ola, 2016). A main component of use in limestone is CaO because it has wide industrial application. Calcium oxide is a major raw material for cement production, fertilizer, paint, and cosmetics production. It also serves as catalyst in the petroleum and biodiesel industries. Calcium oxide is obtained from mineral calcite ($CaCO_3$) as seen in equation (2.1) by calcination at very high temperature ranging from 700 $^oC$ to 1200 $^oC$ for about 2 hrs (Akinniyi and Ola, 2016; Widayat *et al*., 2017). Limestone therefore is a viable source of CaO which is abundant in Nigeria.

$$CaCO_{3(s)} \xrightarrow{\text{Temperature at } 700 - 1{,}200\ ^oC} CaO_{(s)} + CO_{2(g)} \qquad (2.1)$$

### *2.5.3.2 Factors affecting biodiesel production*

Bradley *et al*. (2011) reported that conditions like the choice of catalyst, oil/alcohol ratio, temperature and reaction time affect the yield of biodiesel produced. A minimum stoichiometric ratio of 3:1 for alcohol to oil ratio respectively is required. However, excess alcohol is necessary to drive the reaction close to completion since the reaction is a reversible reaction, this excess alcohol will ensure a forward shift in the equilibrium position as such resulting in biodiesel yield (Krishnakumar and Sivasubramanian, 2017). Farizul *et al*. (2010) stated that it is possible to perform in situ transesterification either at room temperature or at high temperature without tampering with the reaction rate and conversion because the optimal temperature is dependant of feedstock. In the same way, Ismail *et al*. (2013) reported that an increase in the reaction temperature will help shift the equilibrium position to the right as such leading to a successful biodiesel production.

They also stated that an increase in the reaction time in general favours the conversion rate leading to more biodiesel yield however a lengthy reaction time would not result in significant change in the biodiesel conversion process.

## 2.6 Biodiesel Fuel Properties

A typical biodiesel fuel property should conform to the ASTM standards. Table 2.2 shows the ASTM properties for biodiesel.

**Table 2.2:** The American Biodiesel Quality Standard ASTM D6751 (Che *et al*., 2012).

| Property | Method | Limits | Units |
|---|---|---|---|
| Flash point, closed cup | D 93 | 130 mini | ° C |
| Kinematic viscosity, 40 ° C | D 445 | 1.9 – 6.0 | $mm^2/s$ |
| Cetane number | D 613 | 47 mini | |
| Cloud point | D 2500 | - | ° C |
| Carbon residue | D 4530 | 0.050 max | wt.% |
| Acid number | D 664 | 0.80 max | mg KOH/g |
| Free glycerin | D 6584 | 0.020 | wt.% |
| Total glycerin | D 6584 | 0.240 | wt.% |
| Phosphorus | D 4951 | 0.0010 | wt.% |

## 2.7 Optimization of Biodiesel Production

The optimization study is carried out in order to determine how the various process parameters affect the response. The response surface methodology, central composite design is used to carry out the optimization study.

### 2.7.1 Response surface methodology

The RSM is a statistical method which uses quantitative data from appropriate experimental designs to determine and simultaneously solve multivariate equations. This tool can be used in process optimization studies where it serves three primary purposes of; (1) determining the combination of factors which would yield the optimum response;

(2) determining how the response is affected by a given set of factor levels; (3) and describing the interrelationship between the process parameters. Design of Experiment (DOE) is an important aspect of RSM which dictate points at which response is to be evaluated (Cavazzuti, 2013). The response surface experimental designs yield polynomial models which may be first order (linear), second order (quadratic) or third order (cubic). The first order models are described by $2^k$ factorial designs where k is the level of each factor and second order models are described by $2^k$ +2K+1.

### 2.7.2 Central composite design

A 2*k* full factorial to which the central point and the star points are added is known as CCD. The star points refer to the sample points in which all the parameters but one are set at the mean level "*m*". The value of the remaining parameter is given in terms of distance from the central point. An advantage of CCD lies in the fact that it provides information on the response of interest for levels below and above the chosen factor levels (Cavazzuti, 2013).

A five-level-four-factorial CCD using RSM was employed by Goyal *et al*. (2012) to optimize the process variables for minimizing the FFA of jathropha crude oil (JCO) and maximizing the jathropha crude biodiesel (JCB) yield. The high FFA (14.6%) of JCO was reduced to 0.34% by its pre-treatment with methanol (6.5:1) using $H_2SO4$ as catalyst (1.5% v/v) in 125 min time at 50 $^oC$ temperature. Also, JCB yield of 98.3% was achieved with methanol/oil molar ratio (11:1) using NaOH as catalyst (1% w/w) in 110 min time at 55 $^oC$ temperature. Second-order model equations were obtained to predict the FFA content and JCB yield as a function of input parameters. Alhassan *et al*. (2013), used a five-level-three-factor central composite rotable design model of RSM to study the synergistic and antagonistic effects of catalyst concentration, reaction temperature, and

time, using base catalysed transesterification process for production of biodiesel from *gossypium arboreum* seed oil. A predicted yield of 94.93±6.92% for catalyst concentration of 0.53% by weight of the oil, 60 °C for 105 min was obtained using the least square reduced cubic model. The model reliability tests conducted were found to be impressive and conclusively for the optimization of the oil under stated conditions.

CHAPTER THREE
LIST OF PLATES

# 3.0 MATERIALS AND METHODS

## 3.1 Materials and Equipment

The major feedstock used in this research work was orange peel. Orange oil is the primary liquid gotten from the rind of orange (orange peel). Limestone used as source of CaO catalyst was obtained from Obajana in Kogi State. Methanol and all other chemicals were purchased from Hadis and Frankis in Zaria, Kaduna State. Table 3.1 provides a summary of chemicals used in the experimental work which were all of analytical grade. While the list of equipment and apparatus are presented in Table 3.2. All equipment and apparatuses were gotten from chemical engineering lab in Ahmadu Bello University (ABU), Zaria with the exception of electric furnace, which was gotten from metallurgy lab of Federal University of Technology (FUT), Minna.

**Table 3.1:** List of Chemicals used

| S/N | Chemical | Purity Level |
|---|---|---|
| 1 | $H_2SO_4$ | 98 |
| 2 | Methanol | 90 |
| 3 | NaOH | 98 |
| 4 | HCL | 36 |
| 5 | KOH | 98 |
| 6 | Phenolphthalein Indicator | 98 |
| 7 | Ether | 95 |
| 8 | Potassium iodide | 98 |
| 9 | Sodium thiosulphate | 95 |
| 10 | Acetone | 98 |

**Table 3.2:** List of Equipment and Apparatus used

**LIST OF PLATES**

| S/N | Equipment | Model | Manufacturer |
|---|---|---|---|
| 1. | Filter Paper | - | - |
| 2. | Weighing Balance | MT-501 | Metlar |
| 3. | Hot plate with magnetic stirrer | 78HW-1 | SearchTech |
| 4. | Beaker | - | Pyrex England |
| 5. | Measuring Cylinder | Jaytec | Pyrex England |
| 6. | Burrete | - | Pyrex England |
| 7. | Conical Flask | - | Pyrex England |
| 8. | Buchner Funnel | - | - |
| 9. | Centrifuge | GLC-2 | Sorvall |
| 10. | Vacuum Pump | ES50 | SpeediVac |
| 11. | Pipette | - | Pyrex |
| 12. | Round Bottom Flask | - | Pyrex England |
| 13. | Glass Rod | - | - |
| 14. | Thermometer | Deluxe | - |
| 15. | Aluminium Foil | - | - |
| 16. | Electric furnace | - | - |
| 17. | GC-MS Machine | QP-2010 | Labtron |

## 3.2 Methodology

LIST OF PLATES

### 3.2.1 Catalyst preparation

Limestone of 5 kg was collected by hand picking from the site in Obajana, Kogi State as shown in Plate I. It was washed with water to remove surface impurities. These samples were oven dried for 6 hrs at temperature of 150 °C after thorough rinsing with distilled water for further cleansing. Crushing of dried limestone lumps into smaller pieces was done with a jaw crusher as shown in Plate II. Then grinding and sieving of samples into mesh size of 100 µm was done as shown in Plate III. Pulverized limestone sample was stored in an air tight container prior to analysis and further treatment as shown in Plate IV. Pulverized limestone sample was weighed and placed in a crucible and calcined at an already established optimum temperature of 850 °C in a muffle furnace for 4 hrs. (Itodo *et al*., 2017; Akinniyi and Ola, 2016; Widayat *et al*., 2017).


**Plate I:** Lumps of limestone

**Plate II:** Crushed limestone

**Plate III:** Ground limestone

**Plate IV:** Sieved limestone sample

### 3.2.2 Catalyst characterization LIST OF PLATES

The estimation of $CaCO_3$ in the limestone was calculated. The chemical, physical and morphological properties of powdered sample obtained before and after calcination were characterized using Thermo-gravimetric analyses (TGA), X-ray fluorescence (XRF) spectrometry, Scanning Electronic Microscopy (SEM), Fourier Transform Infrared Spectroscopy (FTIR), X-ray diffraction (XRD) and Brunauer, Emmett and Teller (BET) analyses.

#### *3.2.2.1 Estimation of $CaCO_3$ in limestone*

A back titration process was carried out to determine the amount in moles, of $CaCO_3$ present in the limestone sample and the percentage of $CO_2$ evolved from the limestone sample. 2 g of powder limestone was weighed into 80 mL of 1 M HCl solution in a beaker. The solution was heated after the bubbles have settled to allow the escape of $CO_2$ from the solution and to drive the reaction into completion as shown in Equation (3.1). The solution was allowed to cool and then transferred to a 250 mL beaker. 25 mL of the HCl and $CaCO_3$ solution was measured out into a conical flask and three drops of methyl orange added. 0.5 M NaOH solution was poured into 50 mL burette to titrate against the excess HCl solution in the conical flask as shown in Equation (3.2). The titration for each sample was repeated three times and the average volume of NaOH used was recorded.

$$CaCO_3(s) + 2HCl\ (aq)\ (excess) \rightarrow CaCl_2\ (aq) + H_2O\ (l) + CO_2\ (g) \quad (3.1)$$

$$HCl\ (aq)\ (excess) + NaOH\ (aq) \rightarrow NaCl\ (aq) + H_2O\ (1) \quad (3.2)$$

The formula used for the percentage of $CaCO_3$ present in limestone is given in Equation (3.3) as

$$\%\ CaCO_3 = \left(\frac{mass\ of\ CaCo3}{Total\ mass\ of\ limestone\ taken}\right) \times 100 \quad (3.3)$$

### *3.2.2.2 Thermo-gravimetric analysis (TGA)* LIST OF PLATES

The thermal transition and decomposition of catalyst sample was done via TGA analysis using PerkinElmer TGA 4000 instrument. 50 mg each of catalyst samples was placed into the instrument via the top loading pan and covered. Nitrogen gas supply to the instrument was adjusted and purge rate was set to 50 ml/min before analysis was conducted. Samples were analysed at stepwise temperature ranges of 50 °C to 1000 °C and data captured by Pyris software.

### *3.2.2.3 X-ray fluorescence (XRF) spectrometry*

X-rays fluorescent (XRF) analysis was conducted using PANanalytical XRF spectrometer (MiniPal 4). X-RF analysis was carried out by placing 2 g of 100 µm size of the sample on a clean stainless-steel lid which was placed in the cubicle of the spectrometer to determine its elemental composition. When the sample was irradiated by X-rays, the system software measures the individual component wavelengths of the fluorescent emission produced by atoms in the sample and compares to standard wavelengths of atoms of known elements.

### *3.2.2.4 Scanning electron microscope (SEM) analysis*

The physical surface morphology of catalyst sample obtained was examined using LEO S-440 Scanning Electron Microscope. A thin layer of calcium oxide catalyst sample was mounted on an aluminium holder by a double-sided tape. To avoid poor image resolution and discharge of electrostatics, the catalyst sample was coated with gold (Au) to thickness of 1.5 to 3 nm. The test was conducted at different magnifications and data generated was record.

### *3.2.2.5 Fourier transform infra-red (FTIR) Spectroscopy*

The infra-red spectrometer analysis of calcium oxide catalyst was performed using Bruker Alpha II infra-red spectrometer. In carrying out the analysis, the spectrometer was powered and allowed to warm up for 5 minutes. For a reliable analysis, the spectrometer sample press tip and the diamond sampling window were cleaned and made clear of any residue from previous sample which was confirmed by the system software. The sample was then placed on the cleaned crystal window and the overhead press tip adjusted until it exerted the desired pressure on the introduced sample. Transmission spectra of composite films were recorded at ambient temperature. Sample was scanned from 4000 to 400 $cm^{-1}$ with resolution of 0.4 $cm^{-1}$.

### *3.2.2.6 X-ray diffraction (XRD) spectrometry*

First, 2 g sample of size 100 µm was pressed in stainless steel holder and then identification of the crystalline phase was conducted by X-ray diffractor (X′Pert MPD – PAN analytical X-ray B.V.) using Cu-Kα radiation operated at 45 kV, 35 mA in which the incidence angle spanned from 5° to 85°2θ at 0.02°2θ step size with a scan speed of 0.5 s/step. This method was used to obtain a high-quality diffraction data of the sample.

### *3.2.2.7 Brunauer, emmett and teller (BET) analysis*

The BET analysis gives the surface area, pore size and pore volume of the sample. The Quantachrome Instruments Nova 3200e surface area analyser was used to analyse the sample.

### 3.2.3 Extraction of oil from orange peel

Orange peels were collected from a local orange trader at Jebbu market in Bassa, Plateau State, Nigeria. The peels were sun dried for a week as shown in Plate V. The dried orange peels were ground to powder form with a manual grinder as shown in Plate VI. With a

soxhlet extractor, oil was extracted from the powdered orange peels using n-hexane as solvent. The crude orange peel oil was separated from the n-hexane by allowing the oil mixture to stand under a fan for the n-hexane to volatilize to a constant weight of the oil. The oil was then dried in a hot air oven at 60 °C for 1 hr as shown in Plate VII.

**Plate V:** Dried Orange Peel

**Plate VI:** Crushed Orange Peel


**Plate VII:** Orange Oil

### 3.2.4 Characterization of the orange oil

After extraction, the liquid was characterized in order to be sure that the liquid extracted was actually the oil. This involved sense of sight, smell and touch. Outlined below are the tests carried out on the oil.

#### *3.2.4.1 Determination of specific gravity (S.G.) / density*

Specific gravity and density of the oil sample was measured in accordance to the procedure described by standard ASTM D5355-95 (2012) using 25 ml Pycnometer. Dry empty bottle of 25 ml capacity was weighed to give $W_0$ and then filled with the oil and reweighed to give $W_1$. The oil was then substituted with water and reweighed after the

bottle had been washed and dried with the empty weight $W_2$. Specific gravity was then calculated using Equation (3.4):

$$Specific\ gravity = \frac{W_1 - W_o}{W_2 - W_o} \quad (3.4)$$

Where $W_0$ = mass (g) of empty Pycnometer, $W_1$= mass (g) of the Pycnometer filled with sample and $W_2$ = mass (g) of the Pycnometer filled with water

Similarly, the density of the oil was calculated using Equation (3.5)

$$\text{Density } (\rho) \text{ of the oil} = \frac{wieght\ of\ oil}{volume\ of\ oil} \quad (3.5)$$

#### *3.2.4.2 Determination of kinematic viscosity*

A viscometer was inserted into a water bath with a set temperature and left for 30 mins. The biodiesel sample was added to the viscometer and allowed to remain in the bath as long as it reaches the test thermometer. The sample was allowed to flow freely and the time required for the meniscus to pass from the first to the second timing mark was taken using a stop watch. The procedure was conducted according to ASTM D445 and was repeated a number of times and the average value were taken which was then multiplied with the viscometer calibration to give the kinematic viscosity.

#### 3.2.4.3 Determination of flash point

The flash point of the orange oil was tested in accordance to ASTM D93. Sample of orange peel oil was heated in a close vessel and ignited. When the sample burns, the temperature was recorded; the pensky-martens cup tester measures the lowest temperature at which application of the test flame causes the vapour above the sample to ignite. The orange peel oil was placed in a cup in such quantity as to just touch the prescribed mark on the interior of the cup. The cover was then fitted onto the position on the cup and Bunsen burner was used to supply heat to the apparatus at a rate of about 5

$^{o}$C per minute. During heating, the oil was constantly stirred. As the oil approaches its flashing, the injector burner is lighted and injected into the oil container after every 12 second intervals until a distinct flash is observed within the container. The temperature at which the flash occurred was recorded. The above step was repeated three times and the average taken.

#### *3.2.4.4 Determination of ester value*

This is simply the number of mg of potassium hydroxide required to saponify the esters in 1.0 g of the sample expressed in Equation (3.6).

$$Ester\ value = saponifiction\ value - acid\ value \quad (3.6)$$

#### *3.2.4.5 Fourier transform infra-red (FTIR) spectroscopy*

The infra-red spectrometer analysis of orange peel oil was performed using Bruker Alpha II infra-red spectrometer. In carrying out the analysis, the spectrometer was powered and allowed to warm up for 5 mins. For a reliable analysis, the spectrometer sample press tip and the diamond sampling window were cleaned and made clear of any residue from previous sample which was confirmed by the system software. The sample was then placed on the cleaned crystal window and the overhead press tip adjusted until it exerted the desired pressure on the introduced sample. Transmission spectra of composite films were recorded at ambient temperature. Sample was scanned from 4000 to 400 $cm^{-1}$ with resolution of 0.4 $cm^{-1}$.

#### *3.2.4.6 Gas chromatography-mass spectrometry (GC-MS) analysis*

A QP- 2010 model GC-MS machine was used for the characterizations of the orange peel oil. In the conduct of the analysis, 2 µl (micro liters) of the orange peel oil sample was injected into the gas chromatograph with its oven temperature programme between 60 $^{o}$C – 280 $^{o}$C at 5 $^{o}$C/min holding time. The injected sample in the gas chromatograph was

separated on a column. Helium gas was used as the carrier gas and mass selective detector was used for the analyses. The analyses were done in scan mode and the components identified based on software matching with standard mass spectra.

### 3.2.5 Characterization of biodiesel produced

As a way of quality control, biodiesel produced was characterized using American Society for Testing and Materials (ASTM).

#### *3.2.5.1 Determination of specific gravity (S.G.) / density*

Specific gravity and density of the biodiesel sample was measured in accordance to the procedure described by standard ASTM D5355-95 (2012) using 25 ml Pycnometer. Dry empty bottle of 25 ml capacity was weighed to give $W_0$ and then filled with the oil and reweighed to give $W_1$. The oil was then substituted with water and reweighed after the bottle had been washed and dried which then gave a weight $W_2$. Specific gravity was then calculated using Equation (3.7).

$$Specific\ gravity = \frac{W_1 - W_o}{W_2 - W_o} \quad (3.7)$$

Where $W_0$ = mass (g) of empty Pycnometer, $W_1$= mass (g) of the Pycnometer filled with sample and $W_2$ = mass (g) of the Pycnometer filled with water

Similarly, the density of the oil was calculated using Equation (3.8).

$$\text{Density } (\rho) \text{ of the oil} = \frac{wieght\ of\ oil}{volume\ of\ oil} \quad (3.8)$$

#### *3.2.5.2 Determination of kinematic viscosity*

A viscometer was inserted into a water bath with a set temperature and left for 30 min. The biodiesel sample was added to the viscometer and allowed to remain in the bath as long as it reaches the test thermometer. The sample was allowed to flow freely and the time required for the meniscus to pass from the first to the second timing mark was taken using a stop watch. The procedure was conducted according to ASTM D445 and was

repeated a number of times and the average value taken which was then multiplied with the viscometer calibration to give the kinematic viscosity.

### *3.2.5.3 Determination of ocetane number*

Cetane number is a measure of the fuel's ignition delay. Higher cetane numbers indicate shorter times between the injection of the fuel and its ignition. Higher numbers have been associated with reduced engine roughness and with lower starting temperatures for engines.

### *3.2.5.4 Determination of flash point*

The flash point of biodiesel was tested in accordance to ASTM D93. Sample of biodiesel was heated in a close vessel and ignited. When the sample burns, the temperature was recorded; the pensky-martens cup tester measures the lowest temperature at which application of the test flame causes the vapour above the sample to ignite. The biodiesel was placed in a cup in such quantity as to just touch the prescribed mark on the interior of the cup. The cover was then fitted onto the position on the cup and Bunsen burner was used to supply heat to the apparatus at a rate of about 5 $^{o}$C per minute. During heating, the oil was constantly stirred. As the oil approaches its flashing, the injector burner is lighted and injected into the oil container after every 12 second intervals until a distinct flash is observed within the container. The temperature at which the flash occurred was recorded. The above step was repeated three times and the average taken.

### *3.2.5.5 Determination of ester value*

This is simply the number of mg of potassium hydroxide required to saponify the esters in 1.0 g of the sample expressed in Equation (3.9).

$$\text{Ester value} = \text{saponifiction value} - \text{acid value} \quad (3.9)$$

### *3.2.5.6 Fourier transform infra-red (FTIR) Spectroscopy*

The infra-red spectrometer analysis of biodiesel was performed using Bruker Alpha II infra-red spectrometer. In carrying out the analysis, the spectrometer was powered and allowed to warm up for 5 minutes. For a reliable analysis, the spectrometer sample press tip and the diamond sampling window were cleaned and made clear of any residue from previous sample which was confirmed by the system software. The sample was then placed on the cleaned crystal window and the overhead press tip adjusted until it exerted the desired pressure on the introduced sample. Transmission spectra of composite films were recorded at ambient temperature. Sample was scanned from 4000 to 400 $cm^{-1}$ with resolution of 0.4 $cm^{-1}$.

### 3.2.5.6 *GC-MS analysis*

A QP- 2010 model GC-MS machine was used for the characterizations of biodiesel. In the conduct of the analysis, 2 µl (micro litre) of the biodiesel sample was injected into the gas chromatograph with its oven temperature programme between 60 $^{o}$C – 280 $^{o}$C at 5 $^{o}$C/min holding time. The injected sample in the gas chromatograph was separated on a column. Helium gas was used as a carrier gas and mass selective detector was used for the analyses. The analyses were done in scan mode and the components identified based on software matching with standard mass spectra.

### 3.2.6 Optimization of in situ transesterification

Orange peel powder of 25 g was mixed with 50 mL of methanol for 10 mins; 1 g of CaO was added the slurry obtained in a conical flask and placed on a heating mantle heated at 65 $^{o}$C. A magnetic stirrer was used to stir the mixture throughout the process of the situ transesterification as shown in Plate VIII. At the end of reaction, the product was separated from the orange peel cake and catalyst by vacuum-filtering through a Buchner

funnel as shown in Plate IX. The excess methanol was distilled off under vacuum and after the products were centrifuged, it formed two phases whereby the upper layer was biodiesel and the lower layer was glycerol. After removal from the glycerol phase, the biodiesel was collected, weighed, and sent for chromatographic analysis to determine the percentage of methyl ester. This procedure was repeated in batches according to the design of experiment (Juliati *et al*., 2017).

**Plate VIII:** In situ Transesterification

**Plate IX:** Separation Process

### 3.3 Design of Experiment

RSM with five-level-four-factor CCD was applied to optimize the production of biodiesel from orange peel during in situ transesterification reaction using DESIGN EXPERT (Version 7.0.0, Stat Ease, Inc., USA) software. Four factors evaluated in this study are methanol to orange peel ratio, catalyst loading, reaction time and reaction temperature. A total of 30 experiments (24 axial points and 6 centre points) were conducted separately to obtain experimental responses for biodiesel yield. The independent factors used in this study for in situ transesterification of orange peel are given in Table 3.3.

**Table 3.3:** Independent Factors used for CCD in the In-Situ Transesterification of Orange Peel

| Variables | Low | High |
|---|---|---|
| Catalyst wt. (%) | 0.5 | 5.0 |
| Methanol : orange peel | 3:1 | 12:1 |
| Reaction Temperature ($^{o}$C) | 50 | 120 |
| Reaction Time (minutes) | 40 | 160 |

# 4.0 RESULT AND DISCUSSION

This section presents a comprehensive view of the results obtained from the experimental study. It also contains statistical analysis of the results as well as evaluation of the effect of selected process parameter on heterogeneous catalyzed in situ transesterification of the orange peel leading to the formation of biodiesel. The discussion of result is also presented.

## 4.1 Catalyst Preparation and Characterization

The calcium oxide catalyst (CaO) was prepared from limestone by calcining the pulverized limestone ($CaCO_3$) at 850 $^oC$ for 4 hours.

### 4.1.1 Estimation of $CaCO_3$ in limestone

The result for the estimation of $CaCO_3$ in the limestone shows that the limestone sample contains 98.1% $CaCO_3$, indicating that Obajana limestone is of high purity. It also follows the trend of the work of Itodo *et al*., (2017).

### 4.1.2 Thermo-gravimetric analysis (TGA) LIST OF PLATES

The thermal transition and decomposition of the limestone sample is shown on Figure 4.1. The dissociation of limestone ($CaCO_3$) increases as calcination temperature increases.

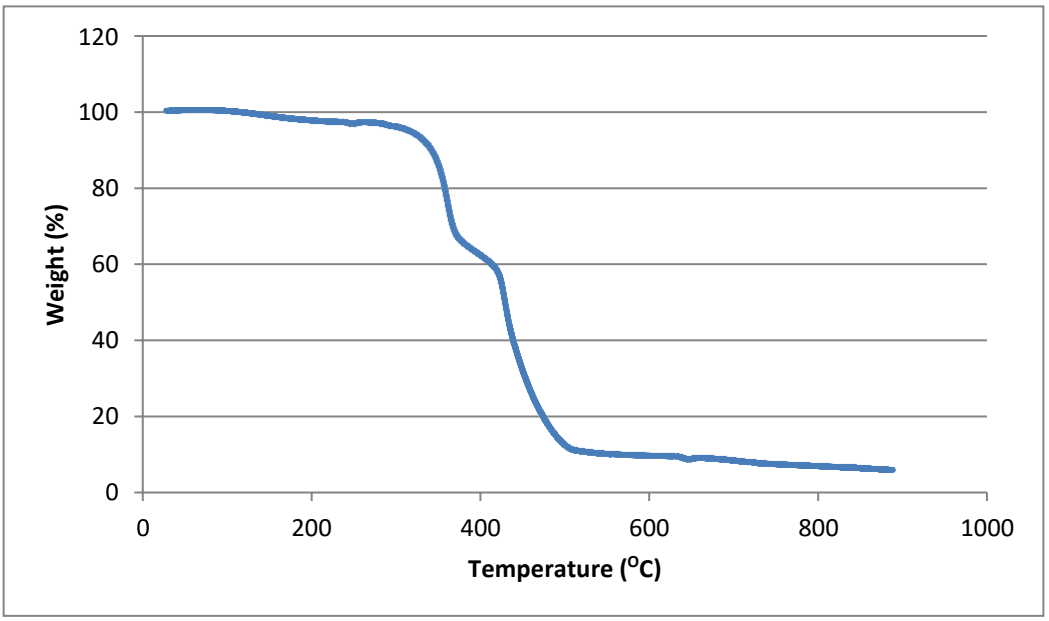


**Figure 4.1:** TGA curve for the Limestone Sample

At temperature range of 33.56 ºC to 228.8 ºC, heat was absorbed by limestone sample to break internal bonding forces as such no visible weight loss was observed. However, as dissociation progresses, a drastic loss of weight from 98 wt(%). to 17 wt(%). was observed at temperature of 300 ºC. Complete dissociation of calcium carbonate was observed at temperature of 550 ºC as shown by the steady state in weight loss of limestone sample as temperature increases above 550 ºC. According to Itodo *et al.* (2017), lime (CaO) of higher purity is usually obtained at temperature above that which complete dissociation took place.

### 4.1.3 X-ray fluorescence (XRF) analysis

The XRF elemental analysis of the limestone as shown on Table 4.1 shows reveals that the limestone sample mainly contains calcium oxide (55.04%), as a major component.

Also present in varying proportions are oxides of silica, aluminum, magnesium, and iron. The loss on ignition (LOI) value of limestone from Obajana is 44.08%. According to Elueze *et al*., (2015), the theoretical LOI value of pure calcium carbonate to weight of carbon dioxide is equal to 44%. Therefore, the nearness of the LOI value (44.08%) of Obajana limestone to the theoretical value indicates its purity.

**Table 4.1:** XRF of the Raw Limestone ($CaCO_3$)

| Composition | Weight (%) |
|---|---|
| CaO | 55.04 |
| MgO | 0.42 |
| $SiO_2$ | 0.35 |
| $Fe_2O_3$ | 0.03 |
| $Al_2O_3$ | 0.06 |
| L.O.I | 44.08 |
| Total | 100.00 |

Indicated on Table 4.2 is the XRF for CaO which shows that CaO is 92.8%, revealing that it is the major component of the limestone. Also present are varying percentages of silica, magnesium, and iron which corresponds with the work of Nurhayati and Utami (2013).

**Table 4.2:** XRF of the Catalyst (CaO)

| Composition | Weight (%) |
|---|---|
| CaO | 92.8 |
| MgO | 0.40 |
| $SiO_2$ | 0.32 |
| $Fe_2O_3$ | 0.03 |
| L.O.I | 6.45 |
| Total | 100.00 |

### 4.1.4 Scanning electron microscopy (SEM) analysis

The SEM micrograph in Figure 4.2 shows the surface morphology of limestone, the absence of pores in the micrograph shows the presence of $CO_2$.

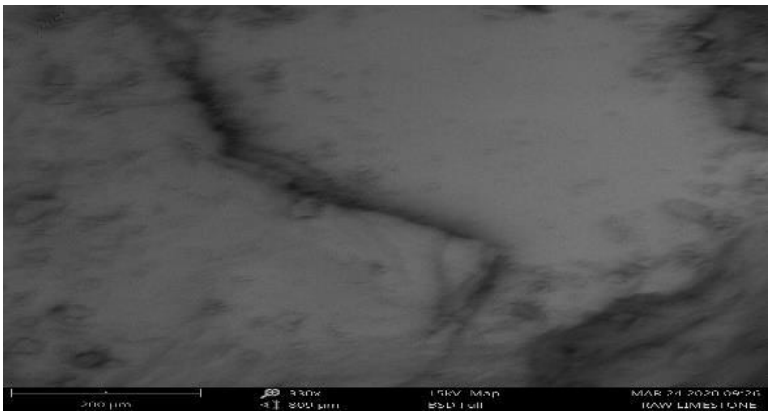

**Figure 4.2:** SEM Micrograph of Raw Limestone

The SEM micrograph in Figure 4.3 shows the honey comb surface morphology of CaO catalyst calcined at 850 $^{o}$C. From the SEM micrograph generated, some crystalline compact particles were observed. Due to the presence of smaller particles with larger surface as observed, the adsorptive capacity of CaO synthesized is high. The micrograph indicates the presence of pores which can be attributed to the release of $CO_2$ as a result of calcination of the limestone. This follows the trend of the work of Bai *et al*. (2009), which shows that the micrograph of CaO indicate grain growth and densification due to high temperature during calcination, the pore radii are therefore moved to larger pores with removal of smaller pores as a result of combination phenomenon which occurs during calcination.

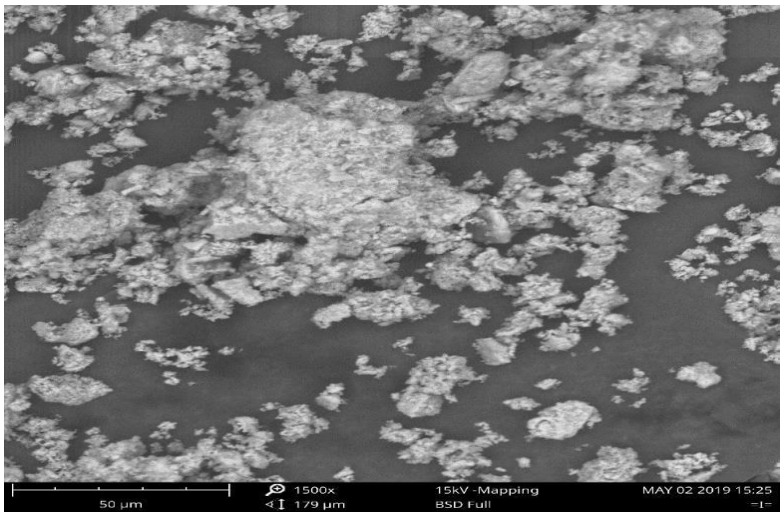


**Figure 4.3:** SEM micrograph of CaO

### 4.1.5 Fourier transform infrared spectroscopy (FTIR) analysis

The peaks of raw limestone and CaO and their key as depicted on Figure 4.4, Table 4.3, and Table 4.4 respectively show the characteristic absorption peaks raw limestone at 1394 $cm^{-1}$, 872 $cm^{-1}$ and 712 $cm^{-1}$. The broad peak at 1394 $cm^{-1}$ shows the asymmetric vibration stretching of the C-O bond which indicates the presence of carbonate. The peaks at 872 $cm^{-1}$ and 712 $cm^{-1}$ show the planar bending of C-O and $CO_3^{2-}$ (Ravisankar *et al*., 2010). The peaks for CaO show characteristic absorption peaks at 3641.6 $cm^{-1}$, 1394 $cm^{-1}$, 872.2 $cm^{-1}$, and 711.9 $cm^{-1}$. The peak at 3641.6 $cm^{-1}$ indicates asymmetric stretching of OH of $Ca(OH)_2$ as the CaO formed rapidly absorbs moisture. The 1394 $cm^{-1}$ indicates the asymmetrical and non-symmetrical C=O attached to the surface of the CaO. The peak at 872 $cm^{-1}$ indicates a planar bending of C-O of the carbonates as a result of the recarbonation of the CaO with $CO_2$ evolved (Ravisankar *et al*., 2010). The $Ca(OH)_2$ formed and recarbonation is observed because the calcination reaction is chemically reversible, quicklime is usually referred to as being highly unstable, the peak at 711$cm^{-1}$ also indicate carbonate group (Mohadi *et al*., 2018).

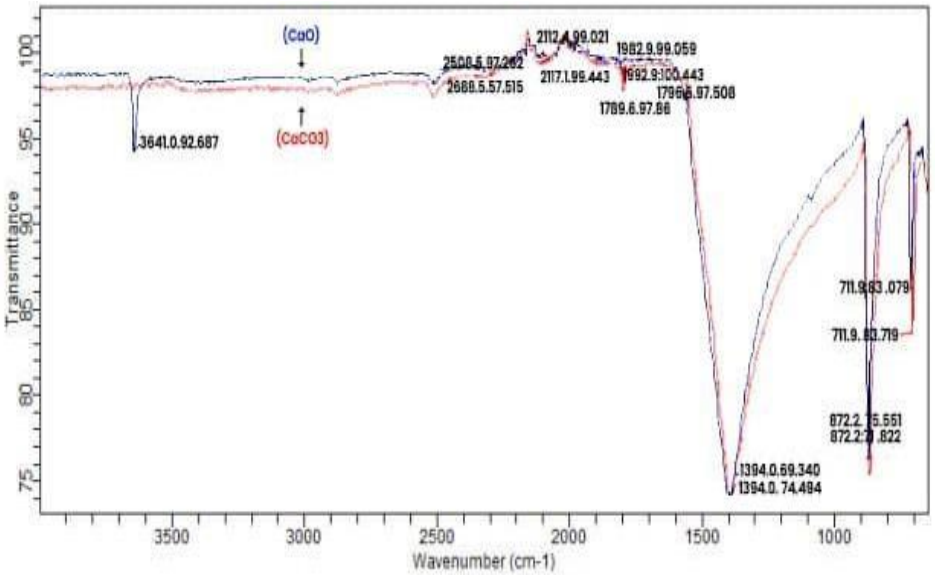


**Figure 4.4:** Superimposed FTIR Spectra for Raw Limestone and CaO

**Table 4.3:** FTIR for Limestone **LIST OF PLATES**

| Peak | Bond | Type | Functional Group |
|---|---|---|---|
| 712 | C-O, $CO_3^{2-}$ | planar bending | Carbonate |
| 872 | C-O, $CO_3^{2-}$ | planar bending | Carbonate |
| 1394 | C-O | asymmetric vibration | Carbonate |

**Table 4.4:** FTIR for CaO

| Peak | Bond | Type | Functional group |
|---|---|---|---|
| 711.9 | C-O | planar bending | Carbonate |
| 872.2 | C-O | planar bending | Carbonate |
| 1394 | C=O | asymmetrical and non-symmetrical | Carbonate |
| 3641.6 | OH | asymmetric stretching | Hydroxide |

### 4.1.6 X-ray diffraction (XRD) spectrometry

The XRD pattern for the raw limestone and CaO is indicated on Figure 4.5. The XRD pattern for limestone recorded its highest peak 29.8 º (d = 0.274 nm) and secondary peaks at 2θ: 22.5 º, and 34.5 º (d = 0.207 nm, and 0.317 nm) typical of calcite the other tertiary peaks at 14 º (d = 0.129 nm), 24 º (d = 0.221 nm), and 25 º (d = 0.230 nm) shows trace amount of kaolin, calcite, and quartz respectively (Itodo *et al*., 2017). The XRD pattern of the calcined limestone shows highest peak at 32.3 º (d = 0. 297 nm), and secondary peaks at 24 º, and 34 º (d = 0.221 nm, and 0.313 nm) shows the presence of CaO and $Ca(OH)_2$ (Itodo *et al*., 2017).

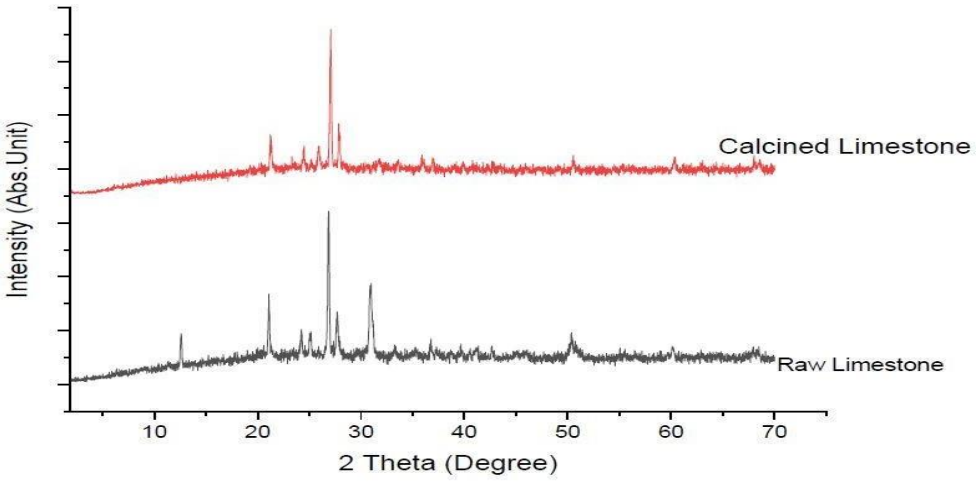


**Figure 4.5:** Superimposed XRD of Limestone and CaO

### 4.1.7 Brunauer, emmett, teller (BET) analysis

The BET analysis of the limestone and CaO is shown on Table 4.5. The result for limestone sample calcined at 850 $^{o}$C shows the pore size and the surface area aid in the viability of the catalyst to be used for the production of biodiesel. It was observed that surface area of limestone sample increases after calcination. According to Itodo *et al.* (2017), a high porous lime (CaO) is produced at temperatures between 800 $^{o}$C and 900 $^{o}$C which represent the most probable temperature for optimum reactivity. Table 4.3 shows the surface area and pore sizes of the limestone and catalyst. The BET analysis revealed that the calcined limestone has a higher surface area, pore volume, and pore size compared to the raw limestone. These properties show the suitability of the calcium oxide as catalyst.

**Table 4.5:** Textural Properties of Raw Limestone ($CaCO_3$) and Catalyst (CaO)

| Sample | Specific Surface area ($m^2/g$) | Pore volume (cc/g) | Pore size (nm) |
|---|---|---|---|
| Raw Limestone | 11.320 | 0.005 | 1.794 |
| C-850 | 25.540 | 0.138 | 1.798 |

## 4.2 Feedstock Quality Characterization

The suitability of a feed stock for biodiesel production relies heavily on its properties. The following results were obtained based on the characterization of the orange peel oil and are shown on Table 4.6.

**Table 4.6:** Characteristics of Orange Peel Oil

| S/N | Property | Unit | Present Study |
|---|---|---|---|
| 1. | Specific Gravity | - | 0.8855 |
| 2. | Kinematic Viscosity | $mm^2/s$ | 1.5 |
| 3. | Flash Point | $^{o}$ C | 235 |
| 4. | Ester value | wt.% | 113.509 |

### 4.2.1 Fourier transform infrared spectroscopy (FTIR) analysis

The FTIR spectra of the orange peel oil are shown on Figure 4.7. The respective broad and sharp peaks at 3324.8 $cm^{-1}$ and 1017 $cm^{-1}$ show the presence of esters and carboxylic acid as shown in Table 4.7.

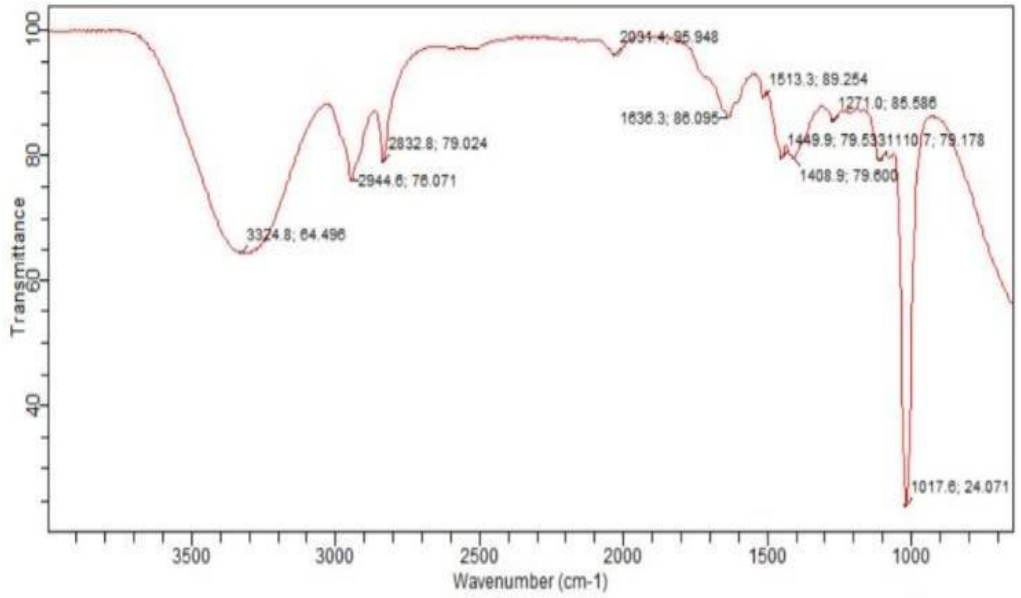


**Figure 4.6:** FTIR of Orange Peel Oil

**Table 4.7:** FTIR for Orange Peel Oil

| Peak | Bond | Type | Functional group |
|---|---|---|---|
| 1017 | O-C | stretch | Carboxylic |
| 3324.8 | =C-H | Sharp | Alkyne |

### 4.2.2 Gas chromatography/mass spectroscopy (GC-MS) analysis of orange peel oil

One of the standards associated with biodiesel synthesis is the composition and structure of the fatty esters comprising the biodiesel. This analysis was carried out using the GC-MS where the relative peak areas in the GC-MS analysis of the components are proportional to the weight proportion of the components (Sokoto *et al*., 2011). The orange peel oil was composed mainly of methyl decanoate, myristate, palmitate, and linoleate. From the GC-MS test analysis of orange peel oil as shown in Table 4.8 and Figure 4.7, shows that the fatty acid profile of orange peel oil ranges from C10 to C36. According to

Agarry *et al*. (2013), oil that contains fatty acids within the range of C16 and C18, have high potential to be used as raw material for the production of biodiesel.

**Table 4.8:** GC-MS profile for orange peel oil

| S/N | Compound | MF | MW | RT | % Peak area |
|---|---|---|---|---|---|
| 1 | D-Limonene | $C_{10}H_{16}$ | 136.23 | 5.54 | 0.09 |
| 2 | Linalool | $C_{10}H_{18}$ | 154.25 | 6.60 | 0.03 |
| 3 | Terpineol | $C_{10}H_{18}O$ | 154.25 | 7.91 | 0.29 |
| 4 | Methyl decanoate | $C_{11}H_{22}O_2$ | 186.29 | 11.82 | 0.05 |
| 5 | Methyl Myristate | $C_{15}H_{30}O_2$ | 242.40 | 13.88 | 0.03 |
| 6 | Methyl palmitate | $C_{17}H_{34}O_2$ | 270.45 | 15.75 | 0.07 |
| 7 | Methyl linoleate | $C_{19}H_{34}O_2$ | 294.50 | 17.21 | 0.07 |
| 8 | 11-Octadecenoic acid, methyl ester | $C_{19}H_{36}O_2$ | 296.50 | 17.25 | 0.08 |
| 9 | Methyl 14-methylheptadecanoate | $C_{19}H_{38}O_2$ | 298.50 | 17.44 | 0.02 |
| 10 | Dodecanoic acid, 1,2,3-propanetriyl ester | $C_{39}H_{74}O$ | 639.00 | 30.63 | 52.21 |
| 11 | Octyl laurate | $C_{20}H_{40}O_2$ | 312.50 | 20.88 | 0.06 |
| 12 | Dodecanoic acid, 1-(hydroxymethyl)-1,2-ethanediyl ester | $C_{27}H_{52}O_5$ | 456.69 | 22.86 | 15.78 |
| | Other compounds | | | | 31.22 |
| | Total | | | | 100.00 |

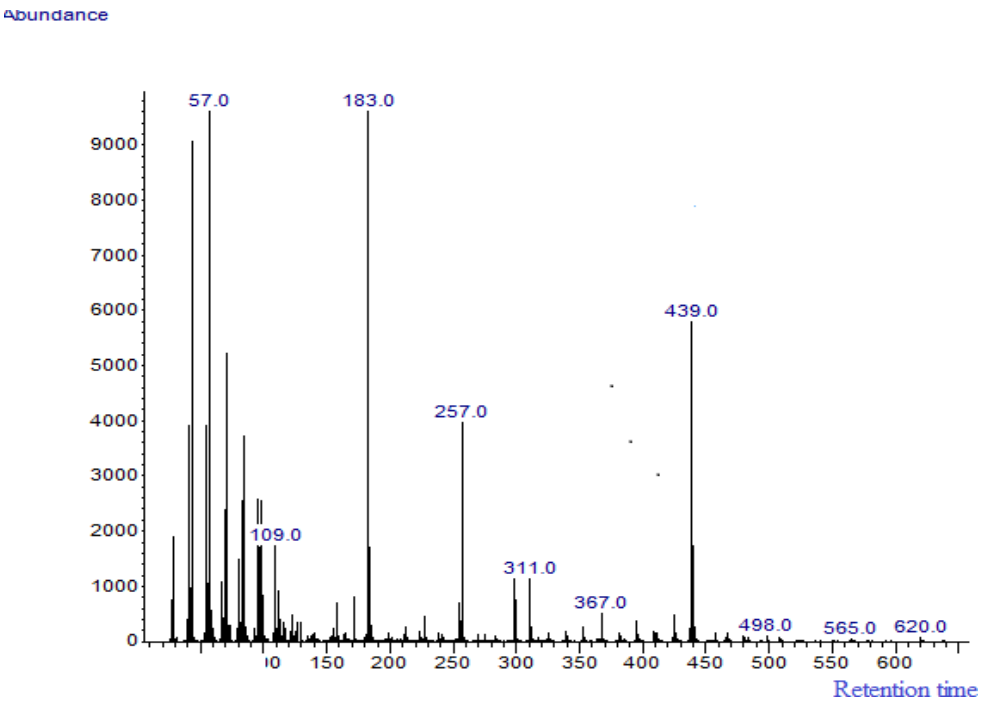


**Figure 4.7:** GC-MS of Orange Peel Oil

### 4.3 Biodiesel Quality Determination

The biodiesel produced is characterized and compared with ASTM standard as shown on Table 4.9. The ASTM D6751 serves as a guideline which provides information on the properties and quality of good biodiesel.

**Table 4.9:** Characterization of Biodiesel produced from Orange Peel

| S/N | Property | Unit | Present study | ASTM standard |
|---|---|---|---|---|
| 1. | Specific Gravity | - | 0.7580 | 0.87-0.90 |
| 2. | Kinematic Viscosity | $mm^2/s$ | 0.8 | 1.9 – 6.0 |
| 3. | Cetane Number | - | 99 | 47 mini |
| 4. | Flash Point | $^o$ C | 135 | 130 mini |
| 5. | Ester value | wt.% | 98.4555 | |

#### 4.3.1 Density

Density or specific gravity has been described as one of the most basic or important parameters of fuel as certain performance indicators such as heating value and cetane number are correlated with it (Yahaya *et al*., 2014). Although the result obtained shows the density of the orange peel biodiesel was averagely low compared to ASTM standard; it also shows the suitability of the biodiesel with regard to ignition delay (Agarry *et al*., 2013). Yahaya *et al*. (2014) also reported low biodiesel density.

#### 4.3.2 Kinematic viscosity

The obtained kinematic viscosity of 0.8 $mm^2/s$ which is low compared to the ASTM standard of 1.9 – 6.0 $mm^2/s$. This can be attributed to the chain length, position, number and nature of double bonds present in the biodiesel from orange peel as observed by Knothe and Steidly, (2005). The low kinematic viscosity obtained as observed by Yahaya *et al.* (2014) indicates the low soot formation tendency and excellent fuel fuel atomisation during high and low temperature operations of orange peel biodiesel. Also, according to

Sanjay (2013), high values of kinematic viscosity give rise to poor fuel atomization, incomplete combustion, and carbon deposition.

### 4.3.3 Cetane number

Cetane number of biodiesel is generally higher than conventional diesel because of its longer fatty acids carbon chains and saturated molecules (El-Shimi *et al*., 2013). Cetane number of orange peel biodiesel was calculated to be 99, which is higher compared to 45.8 for rapeseed biodiesel as carried out by Encinar *et al*., (2010) and also better than 38 as obtained for jatropha biodiesel by Sivaramakrishnan and Ravikumar (2012).

### 4.3.4 Fourier transform infrared spectra (FTIR) analysis

Figure 4.8 and Table 4.10 shows the FTIR spectrum of the biodiesel produced from orange peel. It can be observed that the C-H stretching absorption occurs at wavelength 3339.7 $cm^{-1}$. While the 2920 $cm^{-1}$ and 1013.8 $cm^{-1}$ are associated with -C-H stretch and O-C stretch respectively.

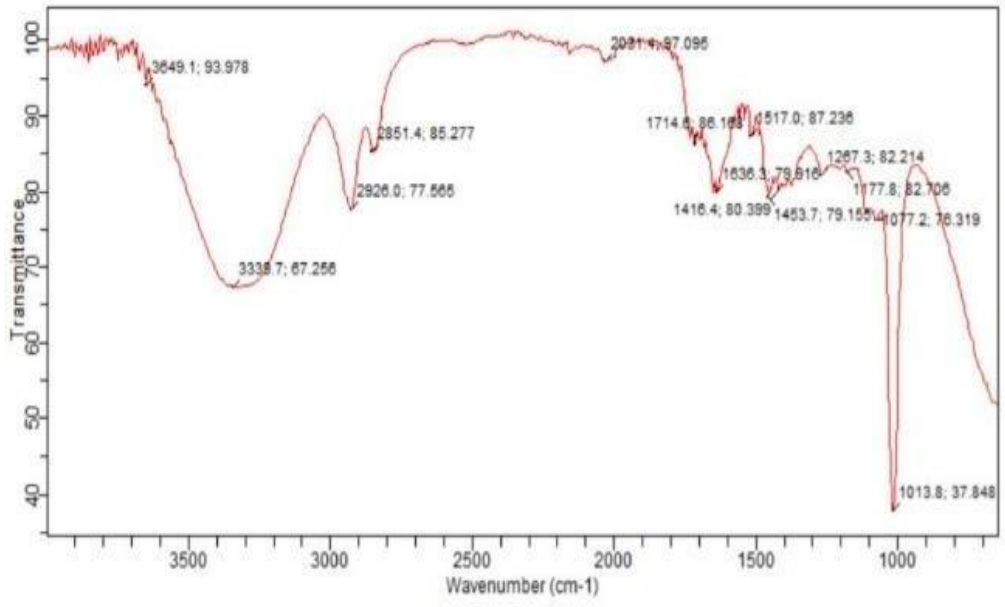


**Figure 4.8:** FTIR Spectra of Biodiesel

**Table 4.10:** FTIR Functional Groups from Orange Peel Biodiesel



| Peak | Bond | Type | Functional Group |
|---|---|---|---|
| 1013.8 | O-C | stretch | RH2C-O |
| 1077 | O-C | stretch | RR'HC-O |
| 1178 | C=O | stretch | Acid |
| 1267.3 | C-C | stretch | Alkane |
| 1453.7 | C-C | stretch | Alkane |
| 1410.4 | C-C | stretch | Alkane |
| 1630.3 | C=C | stretch | Alkene |
| 1714 | C=O | stretch | Acid |
| 2031.4 | C=O | stretch | Anhydride |
| 2851.4 | C-H | stretch | Aldehyde |
| 2920 | C-H | stretch | Alkene |
| 3338.7 | COOH | broad | Acid |
| 3649.1 | COH | broad | Alcohol |

### 4.3.5 GC-MS analysis of the synthesized biodiesel

One of the standards associated with biodiesel synthesis is the composition and structure of the fatty esters comprising the biodiesel. This analysis was carried out using the GC-MS as shown in Figure 4.9 and Table 4.11 where the relative peak areas in the GC-MS analysis of the components are proportional to the weight proportion of the components as indicated by Sokoto *et al*., (2011).

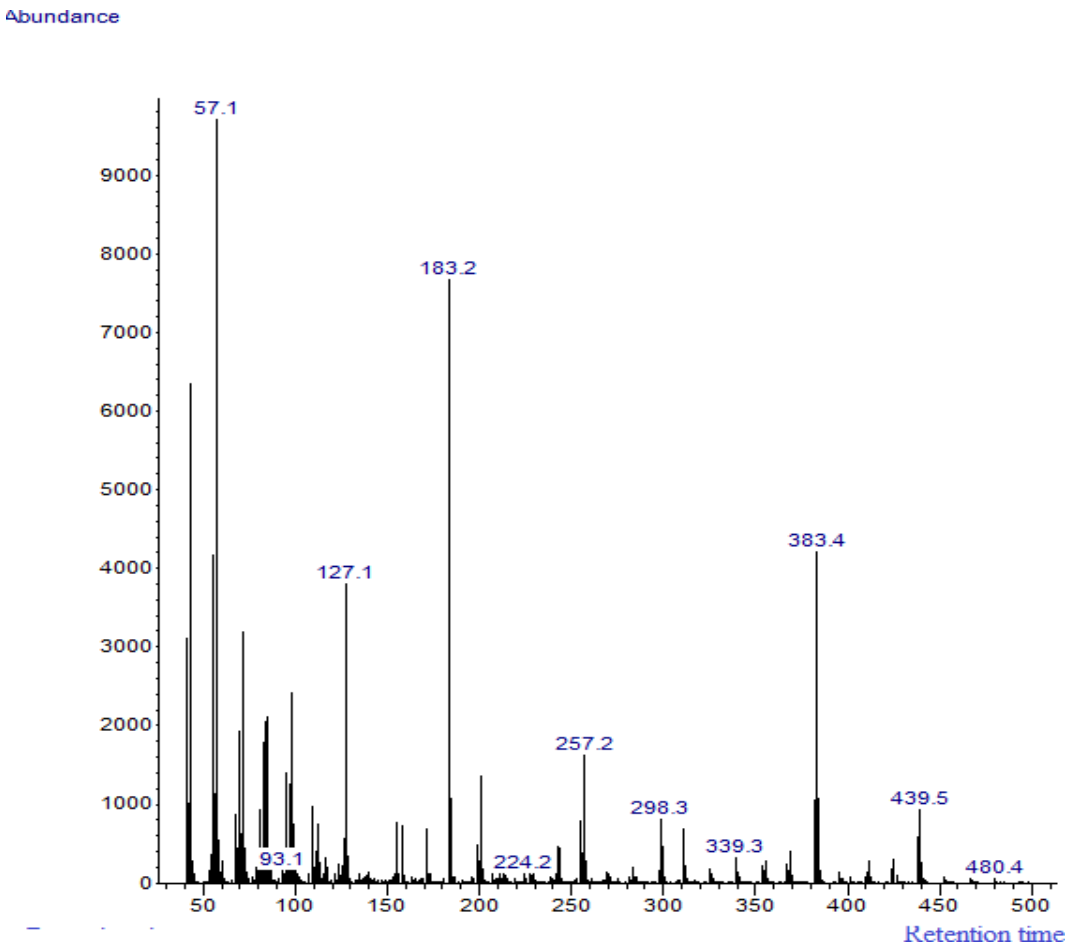


**Figure 4.9:** GC-MS chromatograph of biodiesel

**Table 4.11:** GC-MS Profile for Orange Peel Biodiesel



| FAME | Molecular Formula | Molecular Weight | Retention Time | % Peak Area |
|---|---|---|---|---|
| Methyl octanoate | $C_9H_{18}O_2$ | 158.24 | 6.91 | 0.29 |
| Methyl decanoate | $C_{11}H_{22}O_2$ | 186.29 | 10.72 | 3.37 |
| Methyl laurate | $C_{13}H_{26}O_2$ | 214.34 | 11.91 | 3.02 |
| Dodecanoic acid, 2,3-dihydroxypropyl ester | $C_{15}H_{30}O_4$ | 274.39 | 13.73 | 0.10 |
| Butyl octanoate | $C_{12}H_{24}O_2$ | 200.32 | 13.84 | 0.02 |
| Methyl 14-methylpentadecanoate | $C_{17}H_{34}O_2$ | 270.50 | 15.67 | 0.05 |
| Methyl palmitate | $C_{17}H_{34}O_2$ | 270.45 | 15.83 | 2.30 |
| Isobutyl myritate | $C_{18}H_{36}O_2$ | 284.50 | 17.1 | 0.12 |
| Methyl elaidate | $C_{19}H_{36}O_2$ | 296.50 | 17.33 | 2.85 |
| Methyl stearate | $C_{19}H_{38}O_2$ | 298.50 | 17.5 | 0.67 |
| Glyceryl 1,3-distearate | $C_{35}H_{68}O_5$ | 568.90 | 20.12 | 2.16 |
| 2-Hydroxy oleate | $C_{20}H_{38}O_3$ | 326.52 | 21.65 | 0.033 |
| Octanoic acid, 1-methyltridecyl ester | $C_{22}H_{44}O_2$ | 340.60 | 22.06 | 0.46 |
| Dodecanoic acid, 1-(hydroxymethyl)-1,2-ethanediyl ester | $C_{27}H_{52}O_5$ | 456.69 | 22.65 | 13.57 |
| Dodecanoic acid, 1,2,3-propanetriyl ester | $C_{39}H_{74}O$ | 639.00 | 32.01 | 34.47 |
| Ethyl dodecanoate | $C_{14}H_{28}O_2$ | 228.37 | 30.73 | 9.34 |
| Heptyl palmitate | $C_{23}H_{46}O_2$ | 345.62 | 30.85 | 0.73 |
| Total esters | | | | 73.55 |
| Other compounds | | | | 25.29 |
| Overall total | | | | 98.84 |

From the GC-MS result, it can be seen that the fatty acid composition of orange peel oil biodiesel is dominated by saturated fatty acids which consists of mainly of dodecanoic acid, lauric acid, stearic acid, decanoic acid which is in accordance with past work of Chinnasamy *et al*. (2010) and Velasquez *et al*. (2011).

### 4.4 Optimization of Biodiesel Production from Orange Peel

Optimization of the in situ transesterification process from orange peel was conducted using the DESIGN EXPERT (Version 7.0.0, Stat Ease, Inc., USA) software. The

parameters considered include catalyst loading (A), methanol to orange peel ratio (B), reaction temperature (C), and reaction time (D) as in appendix.

### 4.4.1 Statistical analysis of in situ transesterification reaction of orange peel

The analysis of variance (ANOVA) shown in Table 4.12, Table 4.13, and Table 4.14 was carried out using DESIGN EXPERT (Version 7.0.0, Stat Ease, Inc., USA). The experiments were conducted based on the RSM CCD.

The analysis of the variance (ANOVA) for the response surface quadratic model is shown in Table 4.6. The Model F-value of 2.52 implies the model is significant. The F-value is the ratio of the model SS / residual SS and shows the relative contribution of the model variance to the residual variance. There is only a 4.33% chance that a "Model F-Value" this large could occur due to noise. The model expression developed that relates the biodiesel yield and the four reaction parameters considered (A, B, C, D), was suitable because its p-value is less than 0.05. The significant factors from ANOVA analysis is the binary interaction of methanol to orange peel ratio with a p-value of 0.0023 which is less than 0.05. The other significant factor is the effect of the methanol to orange peel ratio and catalyst loading and the interaction effect of methanol to orange peel ratio and reaction time with p-value of 0.019. The other factors of the model have no statistical significant effect. The value of the coefficient of variation (CV% = 31.31) gives the precision and reliability of the experiment carried out where a lower value of CV% indicates a better precision and reliability of the experiments carried out. The predicted $R^2$ indicates how well a regression model predicts responses from new observations. Adjusted $R^2$ is a modified version of $R^2$ that has been adjusted for a number of predictions. Adequate precision measures the signal to noise ratio. The ratio of 6.726 indicates an adequate signal. This model can be used to navigate the design space. The coefficient estimate represents the expected change in response per unit

change in factor value when all remaining factors are held constant. The intercept in an orthogonal design is the overall average response of all the runs. The coefficients are adjustments around that average based on the factor settings. When the factors are orthogonal the VIFs are 1; VIFs greater than 1 indicate multi-colinearity, the higher the VIF the more severe the correlation of factors. As a rough rule, VIFs less than 10 are tolerable. The regression analysis produced the following coded equation:

Biodiesel Yield = 29.34 -3.27A +2.77B + 0.15C + 1.61D – 1.86AB + 1.29AC -3.00AD – 3.07BC +6.51BD -3.27CD – $1.83A^2$ + $6.92B^2$ – $1.20C^2$ – $1.04D^2$

The linear effect of A and B, the interaction effect of BD and CD and the quadratic effect of $A^2$ and $B^2$ are the general determining factors of in situ transesterification of Orange Peel as they have the larger coefficients.

### 4.4.2 Analysis of variance for in situ transesterification

**Table 4.12:** Analysis of Variance of the In Situ Transesterification of Orange Peel

| Source | Sum of Squares | Df | Mean Square | F Value | P value |
|---|---|---|---|---|---|
| Model | 3454.67 | 14 | 246.76 | 2.52 | 0.0433 |
| A-Catalyst wt. | 257.22 | 1 | 257.22 | 2.63 | 0.126 |
| B-Meth.: Org. peel | 183.54 | 1 | 183.54 | 1.87 | 0.1913 |
| C-Tempt. | 0.51 | 1 | 0.51 | 5.18E-03 | 0.9436 |
| D-Time | 62.37 | 1 | 62.37 | 0.64 | 0.4374 |
| AB | 55.39 | 1 | 55.39 | 0.57 | 0.4638 |
| AC | 26.45 | 1 | 26.45 | 0.27 | 0.611 |
| AD | 144.3 | 1 | 144.3 | 1.47 | 0.2437 |
| BC | 150.37 | 1 | 150.37 | 1.53 | 0.2345 |
| BD | 677.17 | 1 | 677.17 | 6.91 | 0.019 |
| CD | 203.42 | 1 | 203.42 | 2.08 | 0.1702 |
| A^2 | 91.99 | 1 | 91.99 | 0.94 | 0.3479 |
| B^2 | 1312.94 | 1 | 1312.94 | 13.4 | 0.0023 |
| C^2 | 39.34 | 1 | 39.34 | 0.4 | 0.5359 |
| D^2 | 29.89 | 1 | 29.89 | 0.31 | 0.5889 |
| Residual | 1469.74 | 15 | 97.98 | | |
| Lack of Fit | 1133.15 | 10 | 113.31 | 1.68 | 0.2943 |
| Pure Error | 336.59 | 5 | 67.32 | | |
| Cor Total | 4924.41 | 29 | | | |

**Table 4.13: Fit Statistics**

| Std. Dev. | Mean | C.V.% | $R^2$ | Adjusted $R^2$ | Predicted $R^2$ | Adequate Precision |
|---|---|---|---|---|---|---|
| 9.90 | 31.62 | 31.31 | 0.7015 | 0.4230 | -0.4239 | 6.726 |

**Table 4.14: Coefficients in Terms of Coded Factors**

| Factor | Coeff Estimate | Df | Std Error | 95% CI Low | 95% CI High | VIF |
|---|---|---|---|---|---|---|
| Intercept | 29.34 | 1 | 4.04 | 20.72 | 37.95 | |
| A-Catalyst wt. | -3.27 | 1 | 2.02 | -7.58 | 1.03 | 1 |
| B-Meth : Org. peel | 2.77 | 1 | 2.02 | -1.54 | 7.07 | 1 |
| C-Tempt. | 0.15 | 1 | 2.02 | -4.16E+00 | 4.45 | 1 |
| D-Time | 1.61 | 1 | 2.02 | -2.69 | 5.92 | 1 |
| AB | -1.86 | 1 | 2.47 | -7.14 | 3.41 | 1 |
| AC | 1.29 | 1 | 2.47 | -3.99 | 6.56 | 1 |
| AD | -3 | 1 | 2.47 | -8.28 | 2.27 | 1 |
| BC | -3.07 | 1 | 2.47 | -8.34 | 2.21 | 1 |
| BD | 6.51 | 1 | 2.47 | 1.23 | 11.78 | 1 |
| CD | -3.57 | 1 | 2.47 | -8.84 | 1.71 | 1 |
| A^2 | -1.83 | 1 | 1.89 | -5.86 | 2.2 | 1.05 |
| B^2 | 6.92 | 1 | 1.89 | 2.89 | 10.95 | 1.05 |
| C^2 | -1.2 | 1 | 1.89 | -5.23 | 2.83 | 1.05 |
| D^2 | -1.04 | 1 | 1.89 | -5.07 | 2.98 | 1.05 |

## 4.5 The Effect of Interaction between Process Parameters for In Situ Transesterification.

The Three-dimensional response surfaces are plotted on the basis of the generated model equation to investigate the interaction among variables and to determine the optimum condition of each factor for maximum biodiesel yield.

Figure 4.10 represents the 3D plot of the interaction effect of methanol to orange peel ratio and catalyst loading on the biodiesel yield when the other factors are maintained at their centre points. It was observed on the plot increase in catalyst loading to 1.91% (w/w) and corresponding increase in methanol to orange peel ratio to 11.64:1.00 slightly increased the biodiesel yield to 39.31% which was later kept constant even with increase in catalyst loading. This is because at higher catalyst concentration the mixture becomes

too viscous and causes mixing problem (Buasri *et al*., 2013). Also, higher catalyst loading results in catalyst accumulation on the wall of flask which has the tendency to lower the activity (Busari *et al*., 2013).

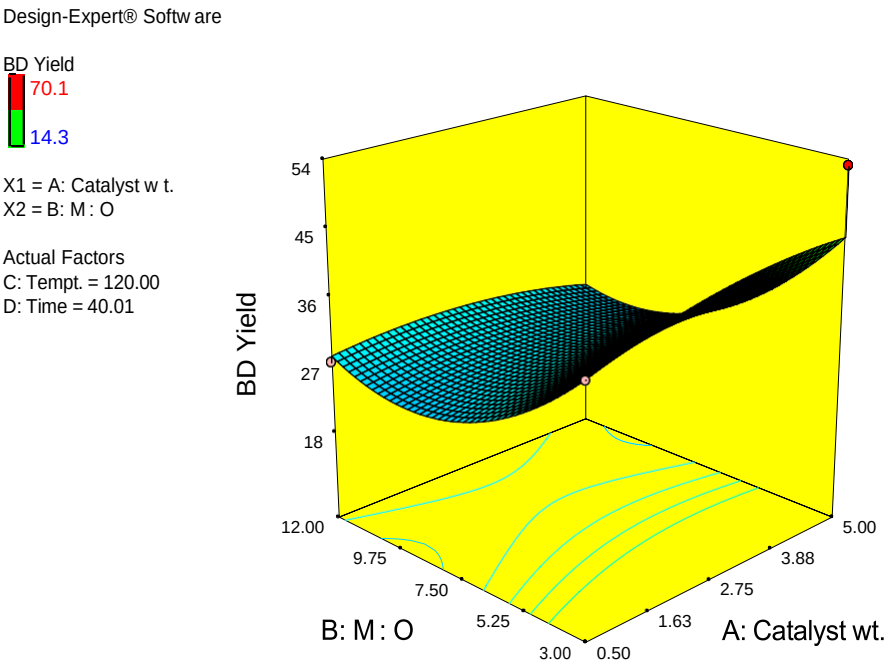


**Figure 4.10:** Response surface plot of the interaction effect of methanol: orange peel ratio and catalyst weight on the biodiesel yield

Figure 4.11 represents the 3D plot of the interaction effect of Reaction Temperature and Methanol to Orange Peel ratio on the Biodiesel yield when the other factors are maintained at their centre points. It can be seen from the Figure that the maximum biodiesel yield of 38.42% was obtained when the temperature was 67.50 $^{o}$C and methanol: oil ratio was 11.50:1.00. The plot shows biodiesel yield decreased steadily with the decrease of methanol to orange peel ratio and continued even with further increase above 11.50:1.00 ratio. It is assumed that the glycerol was mainly dissolved in excessive methanol and thus hinders the reaction of methanol to the reactant and catalyst subsequently interfering with the separation of glycerin (Buasri *et al*., 2013). This results

in dropping the conversion by shifting the equilibrium in the reverse direction (Lim and Lee, 2013).

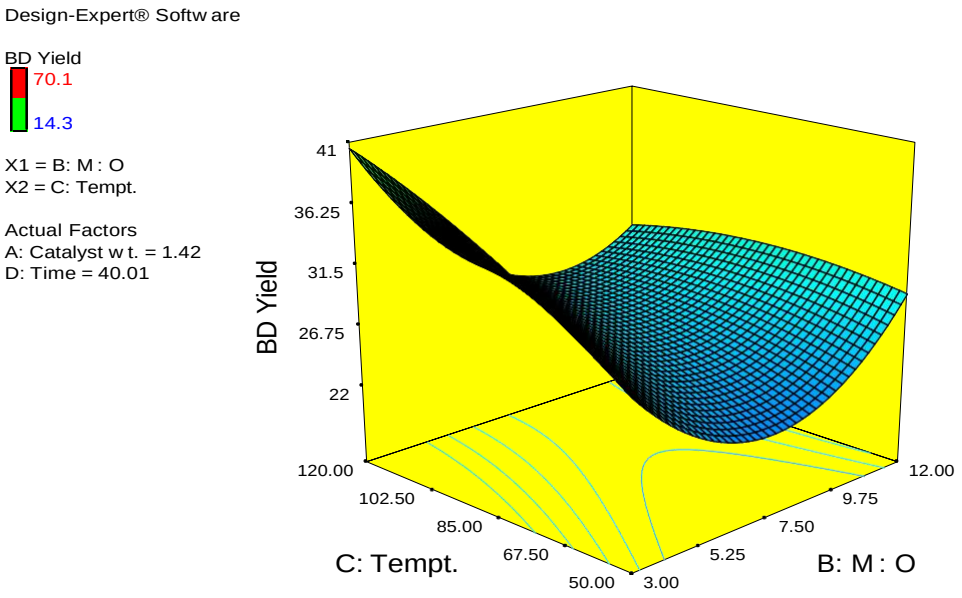


**Figure 4.11:** Response surface plot of the interaction effect of reaction temperature and methanol: oil ratio on the biodiesel yield

Figure 4.12 represents the 3D plot of the interaction effect of reaction time and methanol to orange peel ratio on the biodiesel yield when the other factors are maintained at their centre points. It can be seen from the Figure that the maximum yield biodiesel yield of 29.48% was obtained when the reaction time was 150 min and the methanol: oil ratio was 11.75:1.00. The plot shows the amount of biodiesel yield decreases with decrease methanol and a sharp increase in the biodiesel yield as the amount of methanol increases.

## LIST OF PLATES

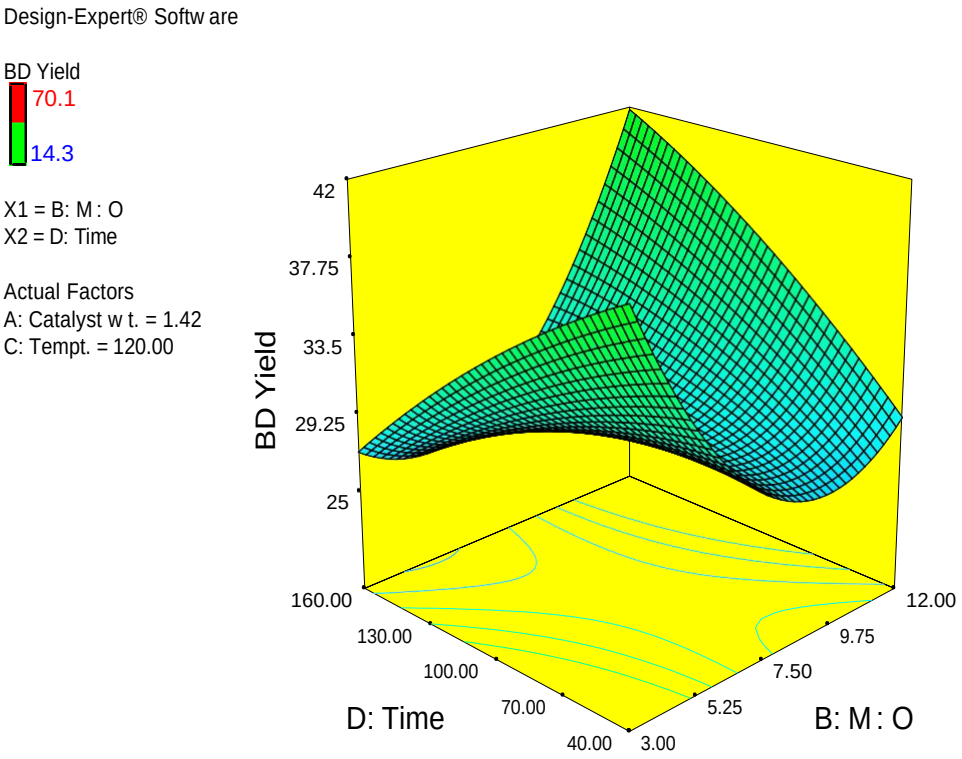


**Figure 4.12:** Response surface plot of the interaction effect of reaction time and methanol: oil ratio on the biodiesel yield

Figure 4.13 represents the 3D plot of the interaction effect of catalyst loading and reaction temperature on the biodiesel yield when the other factors are maintained at their centre points. It can be seen from the Figure that the maximum yield biodiesel yield of 42.78% was obtained when the catalyst loading was 1.91% (w/w) and the temperature was 108.33 $^{o}$C. The plot shows that increase in catalyst loading and temperature leads to increase in biodiesel yield.

## LIST OF PLATES

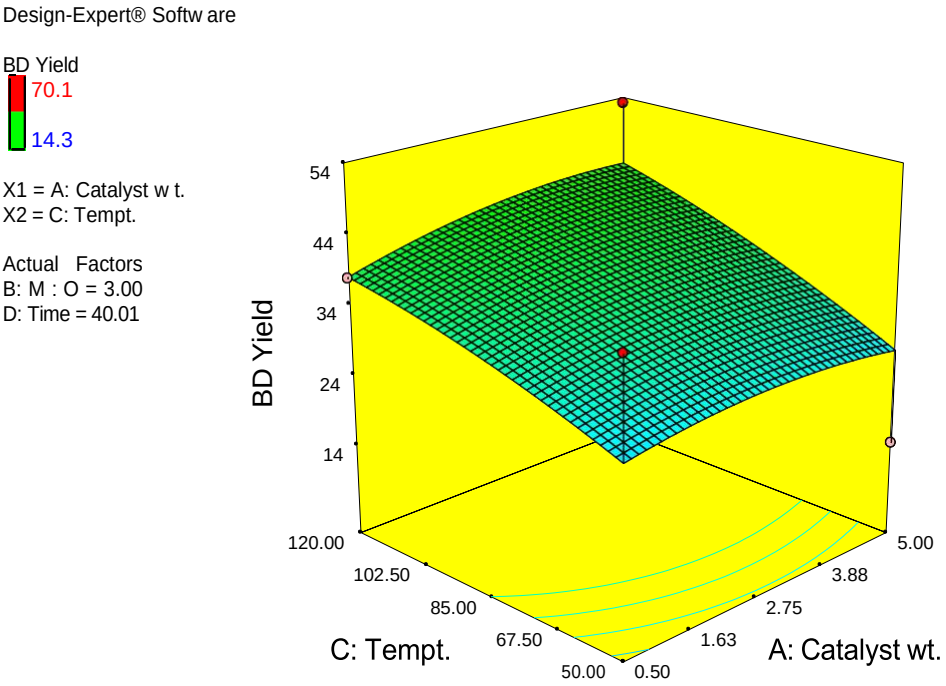


**Figure 4.13:** Response surface plot of the interaction effect of catalyst loading and reaction temperature on biodiesel yield

Figure 4.14 represents the 3D plot of the interaction effect of reaction time and catalyst loading on the biodiesel yield when the other factors are maintained at their centre points. It can be seen from the Figure that the maximum biodiesel yield of 32.26% was obtained when the time was 120 mins and the catalyst loading was 1.63% (w/w). The plot shows that biodiesel yield increases with the increase in reaction temperature; this finding is consistent with the work of Farooq *et al*., (2013). Increase in temperature allows reactant to be more miscible which resulted in higher reaction rate.

## LIST OF PLATES

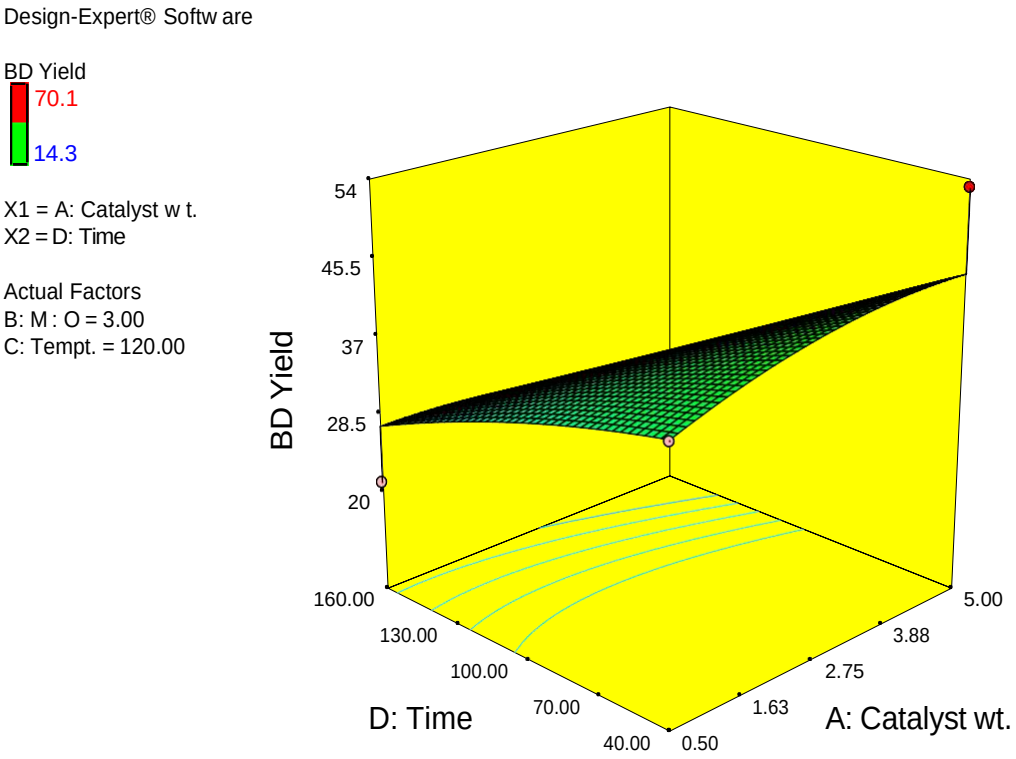


**Figure 4.14:** Response surface plot of the interaction effect of catalyst loading and reaction time on the biodiesel yield

Figure 4.15 represents the 3D plot of the interaction effect of reaction temperature and reaction time on the Biodiesel yield when the other factors are maintained at their centre points. From the Figure, it can be seen that the maximum biodiesel yield of 29.48% was recorded when the reaction temperature was 93.75 $^{o}$C and catalyst weight was 2.38% (w/w). The result shows that biodiesel yield is increasing with the increasing of reaction temperature. This is because high temperature results in increase in miscibility which results in higher reaction rate (Helwani *et al*., 2009).

## LIST OF PLATES

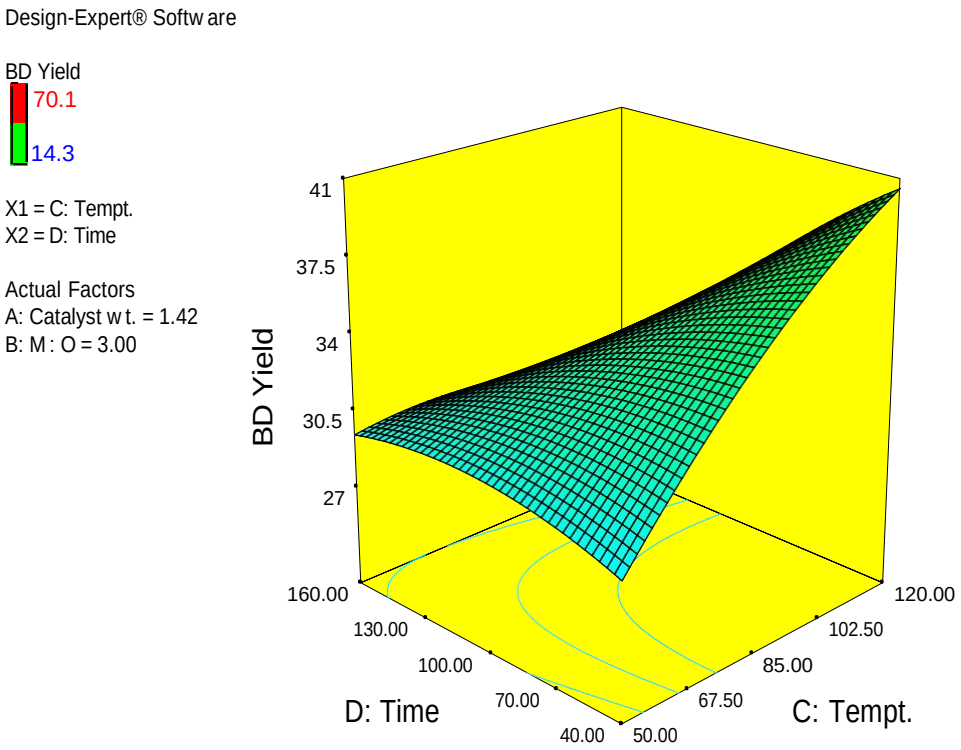


**Figure 4.15:** Response Surface Plot of the Interaction Effect of Reaction Temperature and Reaction Time on the Biodiesel yield

The RSM plots of the interaction effect of the various reaction parameters against Biodiesel yield as represented by Figure 4.10 to 4.15 resulted in different Biodiesel yield results at various operating conditions. However, the optimization solution obtained shows that a biodiesel yield of 70.10% was obtained at a methanol to orange peel ratio of 16.5:1, a catalyst loading of 2.75%, a reaction temperature and time of 85 $^{o}$C and 100 minutes respectively. Velasquez *et al*. (2011) also observed a biodiesel yield of 71.00% at the in situ transesterification of *Chlorella vulgaris*.

Figure 4.16 represents the predicted values versus actual values obtained from the optimization of the in situ transesterification of orange peel oil. The plot shows that the actual values obtained from the study lie close to the regression line as such they correlated with the predicted values generated by design expert. This shows that there is

similarity between the actual and predicted values, this quadratic model is suitable for this study.

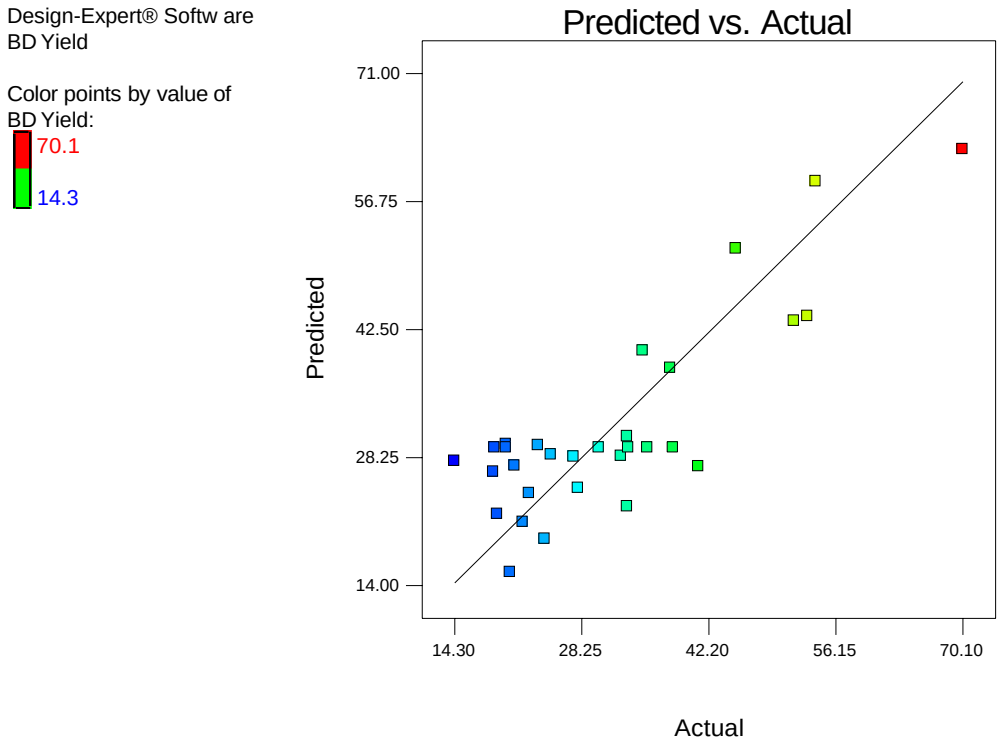


**Figure 4.16:** Predicted values vs. actual values obtained from in situ transesterification of orange peel oil

# 5.0 CONCLUSION AND RECOMMENDATION

## 5. 1 Conclusion

**1** Calcium oxide catalyst was successfully synthesized from Obajana limestone.

**2** The morphology of the CaO showed presence of pores, while size, and surface area were 1.794 nm, and 25.54 $m^2/g$ respectively.

**3** The orange peel oil extracted showed presence of methyl decanoate, myristate, palmitate, and linoleate, indicating its viability for biodiesel production.

**4** The biodiesel produced was characterized with determined properties having values that compared well with the ASTM standards thus making it a recommended fuel for the diesel engine.

**5** Optimization of biodiesel produced was successfully carried out using Design Expert (Version 7.0.0, Stat Ease, Inc., USA) software. The four parameters studied in the in situ transesterification of orange peel resulted in an optimum biodiesel yield of 70. 1 % which was obtained at a methanol to orange peel ratio of 16.5:1, a catalyst loading of 2.75%, a reaction temperature and time of 85º C and 100 minutes respectively.

## 5.2 Recommendation

1 Particle size of orange peel should be put into consideration to aid yield of biodiesel produced.Catalytic performance of CaO can be greatly improved by impregnation or doping with any suitable metal.

2 Funding should be provided by the government as well as the private sector in order to commercialize the production of biodiesel from orange peel.

3 One of the limitations encountered in heterogeneous in situ transesterification is recovery and consequent reuse of catalyst. A means of recovering catalyst should be used in large scale production of heterogeneous based in situ transesterification.

**5.2 Contribution to Knowledge**

Calcium oxide from limestone was used as catalyst for biodiesel production.

After calcination the surface area, pore volume, and pore size of the calcium catalyst increased from 11.32 $m^2/g$ to 25.54 $m^2/g$, 0.05 cc/g to 0.138 cc/g, and 1.794 nm to 1.798 nm respectively. Showing the viability of calcium oxide as a reliable catalyst.

In situ transesterification process was used for orange peel derived biodiesel production and a yield of 70.1% was recorded at an optimized parameter of 100 minutes, 85 $^oC$, catalyst loading of 25%, and methanol to orange peel ratio of 16.5:1.

## LIST OF PLATES REFERENCES


Abdulkareem, A. S., Uthman, H., Afolabi, A. S., & Awonebe, O. L. (2011). Extraction and Optimization of Oil from Moringa Oleifera Seed as an Alternative Feedstock for the Production of Biodiesel. *Journal of Sustainable Growth and Application in Renewable Energy Sources*, 5(5), 243-268. doi:10.5772/25855

Abo, E. S. A., Attia, N. K., El-Ibiari, N. N., El-Diwani, G. I., & El-Khatib, K. M. (2013). In situ Transesterification of Rapeseed and Cost Indicators for Biodiesel Production. *Journal of Renewable and Sustainable Energy Reviews*, 18, 471-477. doi:10.1016/j.rser.2012.10.033

Agarry, S. E., Aremu, M. O., Ajani, A. O., & Aworanti, O. A. (2013). Alkali-Catalysed Production of Biodiesel Fuel from Nigerian Citrus Seeds Oil. *International Journal of Engineering Science and Technology*, 5(9), 1683-1687.

Akinniyi, A. A., & Ola, S. A. (2016). Investigation of certain Engineering properties of some Nigerian limestone deposits for cement production. *Electronic Journal of Geotechnical Engineering*, 21(26), 10471-10482.

Akpan, P. U., Akpan, E. G., & Ozor, P. A. (2014). An Estimation of Orange Oil (Biodiesel) Quantity from Orange Peels in Nigeria. *NIIE 2014 Conference Proceedings*. doi: 10.13140/RG.2.1.3796.2721

Alhassan, Y., Kumar, N., Bugaje, I. M., & Mishra, C. (2013). Optimization of gossypium arboreum seed oil biodiesel production by central composite rotable model of response surface methodology and evaluation of its fuel properties. *Journal of Petroleum Technology and Alternative Fuels*, 5(1), 1-12. doi: 10.5897/JPTAF2013.0093

Amrik, S., & Kumar, G. (2018). Advancement in Catalysts for Transesterification in the Production of Biodiesel: A Review. *Journal of Biochemistry Technology*, 7(3), 1148-1158.

Ani, A. Y., Azlan, M., Ishak, M., & Ismail, K. (2011). Production of Biodiesel via In situ Supercritical Methanol Transesterification, Biodiesel - Feedstocks and Processing Technologies. *Journal of Industrial Technology* 2(3), 4-7. doi:10.5772/59362

Anusi, M. O., Umenweke, G. C., Oyoh, K. B., Nkuzinna, O., & Njoku, C. N. (2018). Characterization of Non-Edible Plants for Biodiesel Production. *American Journal of Engineering Research*, 7(4), 32-36.

Aqliliriana, C. M., Ernee, N. M., & Irmawati, R. (2015). Preparation and characterization of modified calcium oxide from natural sources and their application in the transesterification of palm oil. *International Journal of Scientific and Technology Research*, 4(11), 168-175.

Atabani, A. E., Silitonga, A. S., Anjum, I., Mahlia, T. M. I., Masjuki, H. H., & Mekhilef, S. (2012). A Comprehensive Review on Biodiesel as an Alternative Energy Resource and its Characteristics. *Journal of Renewable and Sustainable Energy Reviews*, 16(4), 2070-2093. doi:10.1016/j.rser.2012.

Bai, H., Shen, X., Liu, X., & Liu, S. (2009). Synthesis of Porous CaO Microsphere and its Application in Catalysing Transesterification Reaction for Biodiesel. *Transaction of Nonferrous Metals Society of China*, 19, 674-677.

Borges, M. E., & Díaz, L. (2012). Recent Developments on Heterogeneous Catalysts for Biodiesel Production by Oil Esterification and Transesterification Reactions: A Review. *Journal of Renewable and Sustainable Energy Reviews*, 16(5), 2839-2849. doi:10.1016/j.rser.2012.01.071

Boro, J., Konwar, L., & Deka, D. (2014). Transesterification of Non-edible Feedstock with Lithium Incorporated Egg Shell Derived CaO for Biodiesel. *United States Department of Agriculture*, 122, 72-78. doi: 10.1016/j.fuproc.2014.01.022

Bradley, D. W., Robert, M. W., & Lance, C. S., (2011). Biodiesel Production by Simultaneous Extraction and Conversion of Total Lipids from Microalgae, Cyanobacteria, and Wild Mixed-Cultures. *Journal of Bioresource Technology*, 102(3), 2724-2730. doi: 10.1016/j.biortech.2010.11.026

Bull, O. S., & Obunwo, C. C. (2014). Biodiesel Production from Oil of Orange (Citrus Sinensis) Peels as Feedstock. *Journal of Applied Science and Environmental Management*, 18(3), 371-374. doi: 10.4314/jasem.v18i3.2

Busari, M. B., Ogbadoyi, E. O., Daudu, O. A. Y., Animashahun, I. M., Yusuf, L., & Lateef, A. A. (2013). Effect of Natural and Combined Fungal Fermentation on Phytate, Tannin and Some Mineral Contents of Corn cobs. *International Journal of Applied Biological Research*, 5(1), 82-89.

Casas, L., Hernandez, C., Mantell, N., & Martinez, O. E. (2015). Filter Cake Oil-Wax as raw Material for the Production of Biodiesel: Analysis of the Extraction Process and the Transesterification Reaction. *Journal of Chemistry*, 2, 1-9. doi: 10.1155/2015/946462

Cavazzuti, M. (2013). Optimization methods: from theory to design. *Scientific and Technological*, 262. doi: 10.1007/978-3-642-31187-1_2

Chattip, P., Prasert, P., Armando, T. Q., Motonobu, G., & Artiwan, S. (2012). Microalgal Lipid Extraction and Evaluation of Single-Step Biodiesel Production. *Engineering Journal*, 16(5), 157-166. doi: 10.4186/ej.2012.16.5.157

Che, F., Sarantopoulos, I., Tsoutsos, T., & Gekas, V. (2012). Exploring a Promising Feedstock for Biodiesel Production in Mediterranean countries: a study on Free Fatty Acid Esterification of Olive Pomace Oil. *Journal of Biomass and Bioenergy*, 36, 427-431. doi: 10.1016/j.biombioe.20011.10.005

Chen, W. H., Chen, C. H., Chang, C. M. J., Chiu, Y. H., & Hsiang, D. (2009). Supercritical Carbon dioxide Extraction of Triglycerides from *Jatropha curcas* L. seeds. *Journal of Supercritical Fluids*, 51, 174–180. doi: 10.1016/j.supflu.2009.08.010

Chinnasamy, S., Bhatnagar, A., Hunt, R. W., & Das, K. C. (2010). Microalgae Cultivation in a Wastewater Dominated by Carpet Mill Effluents for Biofuel Applications. *Bioresource Technology*, 101, 309-3105.

Dale, B. (2008). Biofuels: Thinking Clearly about the Issues. *Journal of Agricultural and Food Chemistry*, 56(11), 3885-3891. doi: 10.1021/jf800250

Davis, R., Aden, A., & Pienkos, P. T. (2011). Techno-economic analysis of autotrophic microalgae for fuel production. *Applied Energy*, 88, 3524-3531. doi: 10.1016/j.apenergy.2011.04.018

Demirbas, A. (2009). Biofuels Securing the Planet's Future Energy Needs. *Energy Conversion and Management*, 50(9), 2239-2249. doi: 10.1016/j.enconman.2009.05.010

Demirbas, A. (2010). Biodiesel for Future Transportation Energy Needs. Energy Sources, Part A: Recovery, Utilization, and Environmental Effect. *Energy Conversion and Management*, 32, 1490-1508. doi:10.1080/.15567030903078335

Dokwadanyi, P. (2011). Production and Characterisation of Biodiesel from Jatropha Curcas and *Ricinus Communis.* B.Eng Project submitted to the Department of Chemical Engineering, Federal university of Technology, Minna, Nigeria. (Unpublished). 1-81

Ehimen, E. A., Sun, Z., & Carrington, G. C. (2012). Use of Ultrasound and Co-Solvent to Increase Biodiesel. *Journal of Procedia Environmental Sciences*, 15, 47-55. doi: 10.1016/j.proenv.2012.05.009

El-Shimi, H. I., Nahed, K. A., El-Sheltawy, S. T., & El-Diwani, G. I. (2013). Biodiesel Production from *Spirulina-Plantensis* Microalgaeby In situ Transesterification Process. *Journal of Sustainable Bioenergy Systems*, 3, 224-233 doi:10.4236/jsbs.2013.33031

Elueze, A. A., Jimoh, A. O., & Aromolaran, O. K. (2015). Compositional characteristics and functional applications of Obajana marble deposit in the precambrian basement complex of central Nigeria. *Ife Journal of Science*, 17(3), 591- 603.

Encinar, J. M., Gonzalez, J. F., Pardal, A., & Martinez, G. (2010). Transesterification of Rapeseed Oil with Methanol in the Presence of Various Co-Solvents. *Third International Symposium on Energy from Biomass and Waste*, 85, 197-203.

Farizul, H. K., Adam, P. H., & Rabitah, Z. (2010). Biodiesel Production by In situ Transesterification: A Review. *Journal of Biofuels*, 1(2), 355-365. doi:10.4155/bfs.10.6

Farooq, M., Ramli, A., & Subbarao, D. (2013). Biodiesel Production from Waste Cooking Oil Using Bifunctional Heterogeneous Solid Catalysts. *Journal of Cleaner Production*, 59, 131-140. doi: 10.1016/j.jclpro.2013.06.015

Fatoye, F. B., & Gideon, Y. B. (2013). Geology and occurrences of limestone and marble in Nigeria. *Journal of Natural Sciences Research*, 3(11), 60-65.

Felix, B. F., & Yomi, B. G. (2013). Geology and Occurrences of Limestone and Marble in Nigeria. *Journal of Natural Sciences Research*, 3(11), 67-69.

Ga, V. K., Woon, Y. C., Do, H. K., Shin, Y. L., & Hyeon, Y. L. (2014). Enhancement of Biodiesel Production from Marine Algae, *Scenedesmus* sp. through In situ

Transesterification Process Assisted by An Acidic Catalyst. *Journal of BioMed Research International*, 2014, 391542. doi:10.1155/2014/391542

Goyal, P., Sharma, M. P., & Siddharth, J. (2012). Optimization of esterification and transesterification of high FFA Jatropha curcas oil using response surface methodology. *Journal of Petroleum Science Research*, 1(3), 36 - 43.

Grana, R., Frassoldati, A., Cuoci, A., Faravelli, T., & Ranzi, E. (2012). A wide range kinetic modelling study of pyrolysis and oxidation of methyl butanoate and methyl decanoate Note I: Lumped kinetic of methyl butanoate and small methyl esters. *Fuel Processing Technology*, 43, 124 - 139.

Gupta, P. K., Kumar, R., Panesar, B. S., & Thapar, V. K. (2007). Parametric Studies on Biodiesel Prepared from Rice Bran Oil. *Agricultural Engineering International*, 59, 346-53. doi: hdl.handle.net/1813/10635

Haas, M. J., & Scott, K. M. (2007). Moisture Removal Substantially Improves the efficiency of In situ Biodiesel Prooduction from Soybeens. *Journal of American Oil Chemists' Society*, 84(2), 197-204. doi: 10.1007/s11746-006-1024-2

Helwani, Z., Othman, M. R., Aziz, N., Kim, J., & Fernando, W. J. N. (2009). Technologies for production of biodiesel focusing on green catalytic techniques: A review. *Journal of Fuel Process Technology*, 90(12), 1502-1514.

Idris, A. M. (2016). The effects of alcohol to oil molar ratios and the type of alcohol on biodiesel production using transesterification process. *Egyptian Journal of Petroleum*, 25, 21-31. doi: 10.1016/j.ejpe.2015.06.007

Ika, A. K., Philippe, E., Muriel, C. O., & Suparno, D. (2016). Simultaneous Solvent Extraction and Transesterification of Jatropha oil for Biodiesel Production, and Potential Application of the obtained cakes for binderless Particleboard. *Journal of Fuel*, 181, 870-877. doi: 10.1016/j.fuel.2016.01.021

Iman, N., Christopher, C., John, B. K., & Fujian, L. (2017). Efficient Transformation of Waste Bone Oil into High Quality Biodiesel via a Synergistic Catalysis of Porous Organic Polymer Solid Acid and Porous y-Al203-K20 Solid Base. *Industrial and Engineering Chemistry Research*, 56(36), 10009-10017. doi: 10.1021/acs.iecr.7b02719

Intergovernmental Panel on Climate Change (2012). Renewable Energy Sources and Climate Change Mitigation: Special Report of the Intergovernmental Panel on Climate Change. Cambridge University Press, Cambridge, MA.

Ismail, H. M., Ngoyo, H. K., Gan, S., Lucchini, T., & Onorati, A. (2013). Development of a reduced biodiesel combustion kinetics mechanism for CFD modelling of a light-duty diesel engine. *Fuel Processing Technology*, 106, 388-400.

Itodo, A. U., Nnamonu, L. A., & Ikape, V. O. (2017). Calcination analysis, characterization and dyestuff adsorption potential of Nigerian limestones. *American Journal of Chemistry and Applications*, 4(1), 6-20.

Jacques, C. V. (2017). Heterogeneous Catalysis on Metal Oxides. *Journal of Catalysis*, 7, 341. doi: 10.3390/catal7110341

Jones, C. S., & Mayfieldt, S. P. (2012). Algae Biofuels: Versatility for the Future of Bioenergy. *Journal of Current Opinion in Biotechnology*, 23(3), 346-351. doi: 10.1016/j.copbio.2011.10.013

Juliati, B. T., Haryo, T. P., Donald, S., & Jamaran, K. (2017). Rapid Biodiesel Production from Palm Kernel Through In situ Transesterification Reaction Using CaO As Catalyst. *International Journal of Applied Chemistry*, 13(3), 631-646.

Kansedo, J., Lee, K. T., & Bhatia, S. (2009). *Cerbera odollam* (sea mango) oil as Promising non-edible Feedstock for Biodiesel Production. *Journal of Fuel*, 88(6), 1148-1150. doi: 10.1016/j.fuel.2008.12.004

Knothe, G., & Steidly, K. S. (2005). Kinematic viscosity of biodiesel fuel component and related compounds: Influence of compound structure and comparison to petrol diesel fuel components. *Journal of Fuel*, 1059-1065.

Krishnakumar, U., & Sivasubramanian, V. (2017). Kinetics study of preparation of Biodiesel from crude rubber oil over a modified heterogeneous catalyst. *Indian Journal of Chemical Technology*, 24(1), 430-434.

Leung, D. Y. C., Xuan, W., & Leung, M. K. H. (2010). A Review on Biodiesel Production using Catalysed Transesterification. *International Journal of Applied Energy*, 87, 1083-1095. doi: 10.1016/j.apenergy.2009.10.006 vol.87

Li, P., Xiaoling, M., Rongxiu, L., & Jianjiang, Z. (2011). In situ Biodiesel Production from Fast-growing and high oil content Chlorella pyrenoidosa in Rice Straw Hydrolysate. *Journal of Biomedicine and Biotechnology*. 2011, 141207. doi:10.1155/2011/141207

Lim, S., & Lee, K. T. (2013). Biodiesel Production using Chemical and Biological Methods - A Review of Process, Catalyst, Acyl Acceptor, Source and Process Variables. *Journal of Applied Energy*, 103, 712-720. doi: 10.1016/j.rser.2014.05.084

Marian, E., & Ihab, H. F. (2014). In situ Transesterification of *Chlorella Vulgaris* Towards Bio-Jet Fuel Production. *International Journal of Engineering and Technical Research*, 2(11), 119-123.

Meo, A., Priebe, X. L., & Weuster-Botz, D. (2017). Lipid production with Trichosporon oleaginosus in a membrane bioreactor using microalgae hydrolysate. *Journal of Biotechnology*, 241, 1-10.

Mohadi, R., Lesbani, A., & Susie, Y. (2013). Preparation and Characterization of Calcium Oxide (CaO) from Chicken Bone. *Journal of Chemistry Progress*, 6(2), 76-80.

Muhammad, C., Mukhtar, M., Isah, U., &. Mamuda, U. (2018). In situ Transesterification of *datura metel* Seed Oil using Cao Derived from Snail Shell as a Catalyst for Biodiesel production. *Trends in Science and Technology Journal*, 3(2B), 797-801.

Nagarajan, S., Chou, S. K., Cao, S. Y., Wu, C., & Zhou, Z. (2012). An Updated Comprehensive Techno-Economic Analysis of Algae Biodiesel. *Journal of Bioresource Technology*, 145, 150-156. doi: 10.1016/j.biortech.2012.11.108

Narasimharao, K., Adam, F. L., & Komam, W. (2007)). Catalysts in Production of Biodiesel: A Review. *Journal of Biobased Materials and Bioenergy*, 1(1): 19-30. doi: 10.1166/jbmb.2007.1976

Ngoya, T. (2015). Study of Biodiesel Production from Waste Vegetable Oil using Eggshell Ash as a Heterogeneous Catalyst. Cape Penninsula University of Technology: Cape Town.

Njoku, V. I., & Evbuomwan, B. O. (2014). Analysis and Comparative Study of Essential Oil Extracted from Nigerian Orange, Lemon and Lime Peels. *Greener Journal of Chemical Science and Technology* 1(1), 6-14.

Nur, S. T., Sarina, S., & Azlin, S. A. (2016). High temperature solid-catalyzed in situ transesterification for biodiesel production. *Journal of Technology, Engineering and Sciences*, 79(5), 607-670. doi: 10.11113/jt.v79.11329.

Nurfitri, I., Maniam, G. P., Noor, H., Yusoff, M., & Ganesan, S. (2013). Potential of Feedstock and Catalysts from Waste in Biodiesel Preparation: A Review. *Journal of Energy Conversion and Management*, 74, 395-402 doi: 10.1016/j.enconman.2013.04.042

Nurhayati, M., & Utami, W. (2013). Mollusk Shell Waste of Anadora Gronasa as a Heterogeneous Catalyst for the Production of Biodiesel. *Prosiding Seminar Nasional Kimia UGM ,* 36-39.

Patrick, S. O., Abdullahi, Z., & Bello, I. S. (2013). Biodiesel Development in Nigeria: Prospects and Challenges. *International Journal of Modern Botany*, 3(1), 4-9. doi: 10.5923/j.ijmb.20130301.02

Poonam, S. N., & Anoop, S. (2010). Production of Liquid Biofuels from Renewable Resources. *Journal of Progress in Energy and Combustion Science*, 37 (1), 52-68. doi: 10.1016/j.pecs.2010.01.003

Ramadhas, A. S., Jayaraj, S., & Muraleedharan, C. (2005). Biodiesel Production from High FFA Rubber Seed Oil. *Journal of Fuel*, 84(4), 335-340. doi: 10.1016/j.fuel.2004.09.016

Ravisankar, R., Senthilkumar, G., Kiruba, S., Chandrasekaran, A., & Jebakumar, P. (2010). Mineral analysis of coastal sediment samples of Tuna, Gujarat, India. *Indian Journal of Science and Technology*, 3(7), 858-862

Refaat, A. A. (2010). Biodiesel Production Using Solid Metal Oxide Catalysts. *International Journal of Environment, Science and Technology*, 8(1), 203-221. doi: 10.1007/BF083326210

Robert, B. L. (2013). The Production of Algal Biodiesel using Hydrothermal Carbonization and In situ Transesterification. Retrieved from: rblevine_1.pdf (umich.edu)

Ryan, M., Satriana, M., Dani, S., & Wirda A. (2013). Effect of Moisture Content and Amount of Hexaneon In situ Transesterification of Jatropha Seeds for Biodiesel Production. *Proceedings of the 3rd Annual International Conference Syiah Kuala University (AIC Unsyiah) 2013 In conjunction with The 2nd International Conference on Multidisciplinary Research (ICMR) 2013.*

Sani, A. M., Muhammad, L. A., Muhammad, M. Bello, S. A., Galadima, A., & Bagudo, A. M. (2018). In situ Transesterification of Cottonseeds Oil (*Gossypium* Spp) Using CaO Derived from Egg Shell as Catalyst. *Physical Science and Biophysics Journal*, 2(1), 000109.

Sanjay, B. (2013). Non-Conventional Seed Oils as Potential Feedstocks for Future Biodiesel Industries: A Brief Review. *Research Journal of Chemical Sciences*, 3(5), 99-103. doi: 10.1080/14786419.2014.881361

Sanjaykumar, D., Swati, S., & Raghunath, P. (2012). Preparation of Biodiesel of Undi seed with In situ Transesterification. *Leonardo Electronic Journal of Practices and Technologies*, 20, 175-182.

Satyanarayana, K. G., Mariano, A. B., & Vargas, J. V. C. (2011). A review on microalgae, a versatile source for sustainable energy and materials. *International Journal of Energy Research*, 35, 291-311. doi 10.1002/er.1695

Satyanarayana, M., & Muraleedharan, C. A (2010). Comparative Study of Vegetable Oil Methyl Esters (Biodiesels). *Journal of Biobased Materials and Bioenergy*, 3(4), 335-341. doi: 10.1016/j.energy.2010.09.050

Sevil, Y., & Pinar, T. (2013). An Alternative Fatty Acid Alkyl Esters Production Method: In situ Transesterification. *Transworld Research Network*, 9, 101-124. doi: 10.1016/j.fuel.2013.01.051.25

Sharma, H., Giriprasad, R., & Goswami, M. (2013). Animal fat processing and its quality control. *Journal of Food Process Technology*, 4, 252-258. doi: 10.4172/2157-7110.1000252.

Sharma, Y. C., & Singh, B. (2009). Development of biodiesel: Current scenario. *Journal of Renewable and Sustainable Energy Reviews*, 13(6-7), 1646-1651. doi: 10.1016/j.rser.2008.08.009

Shiu, P. J., Gunawan, S., Hsieh, W. H., Kasim, N. S., & Ju, Y. H. (2010). Biodiesel production from rice bran by a two-step in situ process. *Journal of Bioresource Technology*, 101, 984-989. doi: 10.1016/j.biortech.2009.011

Sinha, S., Agarwal, A. K., & Garg, S. (2008). Biodiesel Development from Rice Bran Oil: Transesterification Process Optimization and Fuel Characterization. *Journal of Energy Conversion and Management*, 49(5), 1248-1257. doi: 10.1016/j.enconman.2007.08.010

Sivaramakrishnan, K., & Ravikumar, P. (2012). Determination of Cetane Number of Biodiesel and It's Influence on Physical Properties. *Journal of Engineering and Applied Sciences*, 7(2), 205-211.

Sokoto, M. A., Hassan, I. G., Dangoggo, S. M., Ahamad, H. G., & Uba, A. (2011). Influence of Fatty Acid Methyl Esters on Fuel Properties of Biodiesel Production from the seed oil of Curcubitapepo. *Nigerian Journal of Basic and Applied Science*, 19, 81-86.

Taiichiro, H., & Shigenori, M. (2010). Energy Crops for Sustainable Bioethanol Production: Which, Where and How?, Plant Production. *Journal of Science*, 13(3), 221-234. doi: 10.1626/pps.13.221

Tasyurek, M., Acaroglu, M., & Kahraman, A. (2010). The Effects of Storage Conditions on Viscosity of Biodiesel. *Energy Sources, Part A: Recovery, Utilization, and Environmental Effects Journal*, 32(7), 645-656. doi: 10.1080/15567030802606061

The Daily Records Top 10 largest citrus producing countries in the world. The Daily Records Bulletin http://www.thedailyrecords.com/2018-2019-2020-2021/world-famous-top-10-list/world/largest-citrus-producing-countriesworld-statistics-states/6867/

Tiwari, A. K., Kumar, A., & Raheman, H. (2007). Biodiesel production from Jatropha oil (Jatropha Curcas) with high free fatty acids: an optimized process. *Journal of Biomass and Bioenergy*, 31,569-575. doi: 10.1016/j.biombioe.2007.03.003

Tobias, I. N. E., Eke, N. V., Okechukwu, R. I., Nwoguikpe, R. N., & Duru, C. M. (2011). Waste to Wealth: Industrial Raw Materials Potential of Peels of Nigerian Sweet Orange (*citrus sinensis*). *African Journal of Biotech*, 10 (33), 6257-6264. doi: 10.1016/j.biortech.2012.11.108

Tshizanga, N., Aransiola, E. F., & Oyekola, O. (2017). Optimization of biodiesel production from waste vegetable oil and egg shell ash. *South African Journal of Chemical Engineering*, 23, 145-156.

Tsigie, Y. A., Huynh, L. H., Ismadji, S., Engida, A. M., & Ju, Y. H. (2012). In situ Biodiesel Production from Wet Chlorella vulgaris Under Subcritical Condition. *Chemical Engineering Journal*, 213, 104-108. doi: 10.1016/j.cej.2012.09.112

Ummu, K., Heri, S. K., Achmad, R., & Mahfud, M. (2018). Production Biodiesel via In situ Transesterification from *Chlorella* sp. using Microwave with Base Catalyst. *Korean Chemical Engineering Research*, 56(5), 773-778. doi: 10.9713/kcer.2018.56.5.773

United States Department of Agriculture (2013). Coffee: World Markets and Trade in Circular Series. Retrieved from https://www.fas.usda.gov/data/coffee-world-markets-and-trade

United States Department of Agriculture (2018). Citrus: world markets and trade. United States Department of Agriculture, Foreign Agricultural Service https://www.fas.usda.gov/data/citrus-world-markets-and-trade

Usta, N. (2005). An experimental study on performance and exhaust emissions of a diesel engine fuelled with tobacco seed oil methyl ester. *Energy Conversions and Management*, 46(15-16), 2373-2386. doi: 10.1016/j.enconman.2004.12.002

Vafakish, B., & Barari, M. (2017). Biodiesel Production by Transesterification of Tallow Fat Using Heterogeneous Catalysis. *Journal of Chemistry*, 66(1-2), 47-52. doi: 10.15255/kui.2016.002

Veillette, M., Giroir-Fendler, A., Faucheux, N., & Heitz, M. (2017). Esterification of free fatty acids with methanol to biodiesel using heterogeneous catalysts: From model acid oil to microalgae lipids. *Chemical Engineering Journal*, 308,101-109. doi: 10.1016/j.cej.2016.07.061

Velasquez, S. B., Lee, J, G. M., & Hester, A. (2011). Alkaline in situ Transesterification of Chlorella vulgaris. *Journal of Fuels*, 94, 544-550. doi: 10.1016/j.fuel.2011.11.045

Vlontzos, G., & Pardalos, P. M. (2017). Assess and Prognosticate Green House Gas Emissions from Agricultural Production of EU Countries, by Implementing, DEA Window Analysis and Artificial Neutral Networks. *Journal of Renewable and Sustainable Energy Reviews*, 76, 155-162. doi: 10.1016/j.rser.2017.03.054

Widayat, W., Darmawan, T., Hadiyanto, H., & Rosyid, R. A. (2017). Preparation of heterogeneous calcium oxide catalysts for biodiesel production. *International Conference of Energy Sciences*, 315-325.

Yahaya, A., Raghvendra, G., Naveen K., & Idris M. B. (2014). Non-Catalytic In situ transesterification of Citrus Peel Waste into Biodiesel via Supercritical Technology: Optimisation by Response Surface Methodology. *Journal of Biofuels*, 5 (1), 41-52. doi: 10.5958/0976-4763.2014.00006.3

Yoosuk, B., Udomsap, P., Puttasawat, B., & Krasae, P. (2010). Improving Transesterification Activity of Cao with Hydration Technique. *Journal of Bioresource Technology*, 101(10), 3784-3786. doi: 10.1016/j.biortech.2009.12.114

Yusuf, N. N., Kamarudin, S. K., & Yaakub, Z. (2011). Overview on the current trends in biodiesel production. *Journal of Energy Conversion and Management*, 52**,** 2741-2751. doi: 10.1016/j.enconman.2010.12.004

Zeljka, K., Ivana, L., Miodrag, Z., Ljiljiana, M., & Dejan, S. (2016). Calcium Oxide Based catalysts for biodiesel Production: A Review. *Journal of Chemical Industry and Chemical Engineering Quarterly*, 22, 10-10. doi: 10.2298/CICEQ160203010K

## LIST OF APPENDICES

## Appendix A

### I. Characterization of the Feedstock

**Limestone:**

**Determination of percentage $CaCO_3$ in Limestone**

Using the formula% $CaCO_3$ = ( $\frac{mass\ of\ CaCo3}{Total\ mass\ of\ limestone\ taken}$) x 100

( $\frac{0.981}{1}$) x 100 = 98. 1%

**Orange Peel Oil:**

**Determination of Specific Gravity and Density**

Using the formula $Specific\ gravity = (\frac{W_2 - w}{W_1 - w})$

Specific Gravity = $(\frac{65.55 - 30.19}{70.12 - 30.19}) = \frac{35.36}{39.93} = 0.8855$

**Determination of Ester Value**

Using this formula

$$Ester\ value = saponifiction\ value - acid\ value$$

Ester Value = $126.225 - 12.716 = 113.509w\%$

## GC-MS Profile of Orange Peel Oil

**List of Plants**

| PK | RT | Area Pct | Library/ID | Qual |
|---|---|---|---|---|
| 1 | 5.5369 | 0.0859 | D-Limonene | 98 |
| 2 | 6.595 | 0.0312 | Linalool | 96 |
| 3 | 7.9124 | 0.2936 | Terpineol | 90 |
| 4 | 8.2741 | 0.1309 | 2,3-Epoxyhexanol | 38 |
| 5 | 8.387 | 0.0327 | Oxalic acid, cyclohexylmethyl ethyl ester | 27 |
| 6 | 9.5006 | 0.0169 | 3-Penten-2-one, 3-(2-furanyl)- | 25 |
| 7 | 11.8197 | 0.0525 | Dodecanoic acid, methyl ester | 98 |
| 8 | 12.4841 | 0.023 | Dodecanoic acid | 98 |
| 9 | 12.5365 | 0.0101 | Cetene | 92 |
| 10 | 13.8815 | 0.0297 | Methyl tetradecanoate | 98 |
| 11 | 15.7484 | 0.0722 | Hexadecanoic acid, methyl ester | 98 |
| 12 | 17.207 | 0.0692 | 9,12-Octadecadienoic acid (Z,Z)-, methyl ester | 99 |
| 13 | 17.2517 | 0.0838 | 11-Octadecenoic acid, methyl ester | 99 |
| 14 | 17.4426 | 0.0181 | Heptadecanoic acid, 14-methyl-, methyl ester | 97 |
| 15 | 20.6051 | 0.0529 | Lauroyl peroxide | 35 |
| 16 | 20.6978 | 0.0786 | Dodecanoic acid, 1,2,3-propanetriyl ester | 55 |
| 17 | 20.8839 | 0.0622 | Dodecanoic acid, isooctyl ester | 32 |
| 18 | 21.0012 | 0.1459 | Dodecanoic acid, 1-(hydroxymethyl)-1,2-ethanediyl ester | 46 |
| 19 | 21.0358 | 0.0578 | Dodecanoic acid, 1,2,3-propanetriyl ester | 50 |
| 20 | 21.1358 | 0.2627 | Benzamide, 2-bromo-N-[2-(3-fluorophenyl)-5-benzoxazolyl]- | 53 |
| 21 | 21.3468 | 0.5883 | Dodecanoic acid, 1,2,3-propanetriyl ester | 55 |
| 22 | 21.4263 | 0.5311 | Dodecanoic acid, 1,2,3-propanetriyl ester | 38 |
| 23 | 21.6815 | 1.116 | Dodecanoic acid, 1,2,3-propanetriyl ester | 41 |
| 24 | 21.7865 | 0.59 | Dodecanoic acid, 1,2,3-propanetriyl ester | 45 |
| 25 | 22.0347 | 2.4455 | Dodecanoic acid, 1-(hydroxymethyl)-1,2-ethanediyl ester | 59 |
| 26 | 22.2625 | 2.5592 | Dodecanoic acid, 1-(hydroxymethyl)-1,2-ethanediyl ester | 80 |
| 27 | 22.4007 | 1.8003 | Dodecanoic acid, 1,2,3-propanetriyl ester | 46 |
| 28 | 22.593 | 2.9843 | Dodecanoic acid, 1-(hydroxymethyl)-1,2-ethanediyl ester | 84 |
| 29 | 22.6643 | 1.8467 | Benzamide, 2-bromo-N-[2-(3-fluorophenyl)-5-benzoxazolyl]- | 49 |
| 30 | 22.7876 | 1.2551 | Dodecanoic acid, 1-(hydroxymethyl)-1,2-ethanediyl ester | 89 |
| 31 | 22.8072 | 0.364 | Dodecanoic acid, 1,2,3-propanetriyl ester | 60 |
| 32 | 22.9445 | 3.7118 | Benzamide, 2-bromo-N-[2-(3-fluorophenyl)-5-benzoxazolyl]- | 49 |
| 33 | 23.077 | 2.9429 | Dodecanoic acid, 1-(hydroxymethyl)-1,2-ethanediyl ester | 84 |
| 34 | 23.1847 | 1.5379 | Benzamide, 2-bromo-N-[2-(3-fluorophenyl)-5-benzoxazolyl]- | 58 |

| | | | | |
|---|---|---|---|---|
| 35 | 23.2962 | 4.8732 | Benzamide, 2-bromo-N-[2-(3-fluorophenyl)-5-benzoxazolyl]- | 38 |
| 36 | 23.4362 | 1.454 | Dodecanoic acid, 1-(hydroxymethyl)-1,2-ethanediyl ester | 84 |

## LIST OF PLATES

| | | | | |
|---|---|---|---|---|
| 37 | 23.4743 | 0.9887 | Dodecanoic acid, 1-(hydroxymethyl)-1,2-ethanediyl ester | 43 |
| 38 | 23.4955 | 0.9047 | Dodecanoic acid, 1-(hydroxymethyl)-1,2-ethanediyl ester | 62 |
| 39 | 23.5302 | 1.2899 | Dodecanoic acid, 1-(hydroxymethyl)-1,2-ethanediyl ester | 84 |
| 40 | 23.6203 | 1.7129 | Benzamide, 2-bromo-N-[2-(3-fluorophenyl)-5-benzoxazolyl]- | 45 |
| 41 | 23.6395 | 0.9497 | Benzamide, 2-bromo-N-[2-(3-fluorophenyl)-5-benzoxazolyl]- | 41 |
| 42 | 23.6684 | 0.4163 | Benzamide, 2-bromo-N-[2-(3-fluorophenyl)-5-benzoxazolyl]- | 41 |
| 43 | 23.6963 | 1.9456 | Benzamide, 2-bromo-N-[2-(3-fluorophenyl)-5-benzoxazolyl]- | 41 |
| 44 | 23.8099 | 2.9284 | Benzamide, 2-bromo-N-[2-(3-fluorophenyl)-5-benzoxazolyl]- | 35 |
| 45 | 23.8642 | 1.1526 | Fumaric acid, 3,5-difluorophenyl isohexyl ester | 27 |
| 46 | 23.9259 | 1.29 | Lauric anhydride | 14 |
| 47 | 23.9728 | 1.7575 | Dodecanoic acid, 1-(hydroxymethyl)-1,2-ethanediyl ester | 14 |
| 48 | 24.0312 | 1.2521 | Dodecanoic acid, 1,2,3-propanetriyl ester | 18 |
| 49 | 24.059 | 1.0903 | 4-Methoxy-3-nitrobenzyl alcohol | 11 |
| 50 | 24.1059 | 2.0727 | 4-Methoxy-3-nitrobenzyl alcohol | 11 |
| 51 | 24.2075 | 0.9069 | Cyacetacide | 9 |
| 52 | 29.5751 | 0.046 | Heptasiloxane, 1,1,3,3,5,5,7,7,9,9,11,11,13,13-tetradecamethyl- | 38 |
| 53 | 29.7236 | 0.0508 | Dodecanoic acid, 1,2,3-propanetriyl ester | 46 |
| 54 | 30.0456 | 0.276 | Dodecanoic acid, 1,2,3-propanetriyl ester | 94 |
| 55 | 30.2893 | 0.5329 | Dodecanoic acid, 1,2,3-propanetriyl ester | 93 |
| 56 | 30.3909 | 0.1892 | Dodecanoic acid, 1,2,3-propanetriyl ester | 87 |
| 57 | 30.4163 | 0.0647 | Dodecanoic acid, 1,2,3-propanetriyl ester | 93 |
| 58 | 30.8366 | 1.6717 | Dodecanoic acid, 1,2,3-propanetriyl ester | 93 |
| 59 | 30.8742 | 0.176 | Dodecanoic acid, 1,2,3-propanetriyl ester | 93 |
| 60 | 30.9171 | 0.2844 | Dodecanoic acid, 1,2,3-propanetriyl ester | 93 |
| 61 | 30.9452 | 0.4612 | Dodecanoic acid, 1,2,3-propanetriyl ester | 93 |
| 62 | 31.2943 | 1.6994 | Dodecanoic acid, 1,2,3-propanetriyl ester | 91 |
| 63 | 31.35 | 0.4064 | Dodecanoic acid, 1,2,3-propanetriyl ester | 91 |
| 64 | 31.4972 | 1.1777 | Dodecanoic acid, 1,2,3-propanetriyl ester | 93 |
| 65 | 31.5303 | 0.8212 | Dodecanoic acid, 1,2,3-propanetriyl ester | 93 |
| 66 | 31.6317 | 0.2976 | Dodecanoic acid, 1,2,3-propanetriyl ester | 93 |
| 67 | 31.7568 | 1.1044 | Dodecanoic acid, 1,2,3-propanetriyl ester | 93 |
| 68 | 31.7835 | 0.357 | Dodecanoic acid, 1,2,3-propanetriyl ester | 93 |
| 69 | 31.8156 | 0.3048 | Dodecanoic acid, 1,2,3-propanetriyl ester | 93 |
| 70 | 31.8376 | 0.2588 | Dodecanoic acid, 1,2,3-propanetriyl ester | 93 |
| 71 | 31.8659 | 0.4129 | Dodecanoic acid, 1,2,3-propanetriyl ester | 91 |
| 72 | 31.9572 | 0.9036 | Dodecanoic acid, 1,2,3-propanetriyl ester | 91 |

| | | | | |
|---|---|---|---|---|
| 73 | 32.0858 | 1.4438 | Dodecanoic acid, 1,2,3-propanetriyl ester | 91 |
| 74 | 32.1212 | 0.543 | Dodecanoic acid, 1,2,3-propanetriyl ester | 91 |
| 75 | 32.2458 | 1.3184 | Dodecanoic acid, 1,2,3-propanetriyl ester | 91 |

| | | | | |
|---|---|---|---|---|
| 76 | 32.2988 | 0.6723 | Dodecanoic acid, 1,2,3-propanetriyl ester | 93 |
| 77 | 32.3174 | 0.9979 | Dodecanoic acid, 1,2,3-propanetriyl ester | 93 |
| 78 | 32.4546 | 1.0707 | Dodecanoic acid, 1,2,3-propanetriyl ester | 93 |
| 79 | 32.486 | 0.3876 | Dodecanoic acid, 1,2,3-propanetriyl ester | 93 |
| 80 | 32.5624 | 1.1934 | Dodecanoic acid, 1,2,3-propanetriyl ester | 93 |
| 81 | 32.6247 | 1.1167 | Dodecanoic acid, 1,2,3-propanetriyl ester | 93 |
| 82 | 32.6561 | 0.9371 | Dodecanoic acid, 1,2,3-propanetriyl ester | 91 |
| 83 | 32.7199 | 0.2413 | Dodecanoic acid, 1,2,3-propanetriyl ester | 91 |
| 84 | 32.7796 | 0.9588 | Dodecanoic acid, 1,2,3-propanetriyl ester | 93 |
| 85 | 32.8466 | 1.0585 | Dodecanoic acid, 1,2,3-propanetriyl ester | 93 |
| 86 | 32.8638 | 0.2468 | Dodecanoic acid, 1,2,3-propanetriyl ester | 93 |
| 87 | 32.9457 | 1.4958 | Dodecanoic acid, 1,2,3-propanetriyl ester | 93 |
| 88 | 33.072 | 2.194 | Dodecanoic acid, 1,2,3-propanetriyl ester | 91 |
| 89 | 33.157 | 1.3736 | Dodecanoic acid, 1,2,3-propanetriyl ester | 93 |
| 90 | 33.2388 | 1.7327 | Dodecanoic acid, 1,2,3-propanetriyl ester | 93 |
| 91 | 33.2775 | 0.6685 | Dodecanoic acid, 1,2,3-propanetriyl ester | 93 |
| 92 | 33.297 | 0.6947 | Dodecanoic acid, 1,2,3-propanetriyl ester | 93 |
| 93 | 33.3543 | 0.7818 | Dodecanoic acid, 1,2,3-propanetriyl ester | 91 |
| 94 | 33.374 | 1.0445 | Dodecanoic acid, 1,2,3-propanetriyl ester | 93 |
| 95 | 33.4259 | 0.3095 | Dodecanoic acid, 1,2,3-propanetriyl ester | 91 |
| 96 | 33.4588 | 1.0015 | Dodecanoic acid, 1,2,3-propanetriyl ester | 91 |
| 97 | 33.555 | 1.61 | Dodecanoic acid, 1,2,3-propanetriyl ester | 91 |
| 98 | 33.6169 | 2.9291 | Dodecanoic acid, 1,2,3-propanetriyl ester | 91 |
| 99 | 33.7144 | 0.6589 | Dodecanoic acid, 1,2,3-propanetriyl ester | 91 |
| 100 | 33.7865 | 2.3914 | Dodecanoic acid, 1,2,3-propanetriyl ester | 91 |
| 101 | 34.0793 | 1.2589 | 1H-Azonine, octahydro- | 7 |
| 102 | 34.2058 | 3.3042 | Dodecanoic acid, 1,2,3-propanetriyl ester | 38 |

**II. Characterization of Biodiesel produced from the Orange peel**

**Determination of Kinematic Viscosity**

K.v = 0.8 $mm^2/s$

**Determination of Cetane Number**

Using this formula $= 46.3 + (\frac{5458}{s.v}) - (0.225 \times i.v)$

Orange peel BD$= 46.3 + (\frac{5458}{49}) - (0.225 \times 6.5353) = 99.96$

## GC-MS Profile of Biodiesel

**LIST OF PLATES**

| PK | RT | Area Pct | Library/ID | Quality |
|---|---|---|---|---|
| 1 | 6.6252 | 0.0245 | Linalool | 96 |
| 2 | 6.9063 | 0.2858 | Octanoic acid, methyl ester | 94 |
| 3 | 7.9417 | 0.1174 | Terpineol | 90 |
| 4 | 9.5416 | 0.3507 | Decanoic acid, methyl ester | 97 |
| 5 | 11.9074 | 3.0219 | Dodecanoic acid, methyl ester | 97 |
| 6 | 12.119 | 0.0036 | Dodecanoic acid | 97 |
| 7 | 12.4035 | 0.1014 | Dodecanoic acid | 98 |
| 8 | 12.6554 | 0.2563 | Dodecanoic acid | 99 |
| 9 | 12.7954 | 0.0063 | Dodecanoic acid | 96 |
| 10 | 13.5493 | 0.0568 | n-Hexadecanoic acid | 50 |
| 11 | 13.7261 | 0.0963 | Dodecanoic acid, 2,3-dihydroxypropyl ester | 27 |
| 12 | 13.837 | 0.02 | Octanoic acid, 2-butyl ester | 38 |
| 13 | 13.9721 | 2.3468 | Methyl tetradecanoate | 98 |
| 14 | 14.4514 | 0.238 | Tetradecanoic acid | 97 |
| 15 | 14.5509 | 0.2876 | Tetradecanoic acid | 97 |
| 16 | 14.703 | 0.0111 | Nonadecanoic acid | 22 |
| 17 | 15.3491 | 0.1122 | 15-Hydroxypentadecanoic acid | 58 |
| 18 | 15.4632 | 0.0403 | Tetradecanoic acid | 90 |
| 19 | 15.5985 | 0.0476 | cis-Vaccenic acid | 95 |
| 20 | 15.6666 | 0.0549 | Pentadecanoic acid, 14-methyl-, methyl ester | 50 |
| 21 | 15.8318 | 2.3045 | Hexadecanoic acid, methyl ester | 98 |
| 22 | 16.356 | 0.2711 | n-Hexadecanoic acid | 99 |
| 23 | 16.6415 | 0.0517 | Pentadecanoic acid | 94 |
| 24 | 16.738 | 0.0506 | n-Hexadecanoic acid | 98 |
| 25 | 17.099 | 0.1155 | Myristic acid isobutyl ester | 52 |
| 26 | 17.3288 | 2.8546 | 9-Octadecenoic acid (Z)-, methyl ester | 99 |
| 27 | 17.4959 | 0.6688 | Methyl stearate | 99 |
| 28 | 17.8503 | 0.0349 | cis-Vaccenic acid | 95 |
| 29 | 17.8751 | 0.0376 | 9-Octadecenoic acid | 96 |
| 30 | 17.9791 | 0.0261 | cis-Vaccenic acid | 96 |
| 31 | 18.6956 | 0.0344 | 6-Octadecenoic acid, (Z)- | 87 |
| 32 | 18.8147 | 0.0803 | 6-Octadecenoic acid, (Z)- | 47 |
| 33 | 18.9499 | 0.1074 | Glycerol 1-palmitate | 64 |
| 34 | 19.0199 | 0.0461 | 6-Octadecenoic acid, (Z)- | 62 |
| 35 | 19.7806 | 0.0564 | Oleic Acid | 96 |
| 36 | 20.1186 | 2.1585 | Octadecanoic acid, 2-hydroxy-1,3-propanediyl ester | 43 |

| | | | | |
|---|---|---|---|---|
| 37 | 20.4256 | 0.0887 | 15-Hydroxypentadecanoic acid | 53 |
| 38 | 21.6483 | 0.0326 | 9-Octadecenoic acid (Z)-, 2-hydroxyethyl ester | 96 |
| 39 | 22.0353 | 0.2645 | Octanoic acid, 1-methyltridecyl ester | 25 |
| 40 | 22.0787 | 0.1911 | Octanoic acid, 1-methyltridecyl ester | 25 |
| 41 | 22.2409 | 0.0967 | 2-(Decanoyloxy)propane-1,3-diyl dioctanoate | 91 |
| 42 | 22.3423 | 0.3551 | 1-[p-Bromophenyl]-4-nitro-1,3-butadiene | 93 |

## LIST OF PLATES

| | | | | |
|---|---|---|---|---|
| 43 | 22.651 | 2.8633 | Dodecanoic acid, 1-(hydroxymethyl)-1,2-ethanediyl ester | 86 |
| 44 | 22.8788 | 0.0847 | Dodecanoic acid, 1,2,3-propanetriyl ester | 47 |
| 45 | 23.4246 | 0.7233 | Octanoyl chloride | 25 |
| 46 | 24.8176 | 4.3728 | Diethylmalonic acid, 3,4-difluorobenzyl hexyl ester | 45 |
| 47 | 25.1832 | 3.6988 | Dodecanoic acid, ethenyl ester | 38 |
| 48 | 25.8587 | 0.045 | Octadecane, 1-(ethenyloxy)- | 53 |
| 49 | 27.5247 | 2.6896 | Dodecanoic acid, 1-(hydroxymethyl)-1,2-ethanediyl ester | 47 |
| 50 | 28.2685 | 12.5653 | 3-Dibenzofuranamine | 46 |
| 51 | 28.4193 | 4.0344 | Fumaric acid, 3,5-dichlorophenyl isohexyl ester | 47 |
| 52 | 30.8469 | 0.7343 | Hexadecanoic acid, heptyl ester | 18 |
| 53 | 32.755 | 12.9178 | Dodecanoic acid, 1,2,3-propanetriyl ester | 45 |
| 54 | 33.0119 | 8.3537 | Dodecanoic acid, 1,2,3-propanetriyl ester | 46 |
| 55 | 33.1657 | 5.1493 | Dodecanoic acid, 1-(hydroxymethyl)-1,2-ethanediyl ester | 49 |
| 56 | 33.2509 | 3.2244 | Dodecanoic acid, 1,2,3-propanetriyl ester | 46 |
| 57 | 33.3515 | 3.2154 | Dodecanoic acid, 1,2,3-propanetriyl ester | 47 |
| 58 | 33.3911 | 2.2036 | Dodecanoic acid, 1,2,3-propanetriyl ester | 43 |
| 59 | 33.4509 | 1.0186 | Dodecanoic acid, ethenyl ester | 43 |
| 60 | 33.4813 | 2.8669 | Dodecanoic acid, 1-(hydroxymethyl)-1,2-ethanediyl ester | 46 |
| 61 | 33.5708 | 4.6192 | Dodecanoic acid, ethenyl ester | 30 |
| 62 | 33.695 | 0.7577 | Dodecanoic acid, 1,2,3-propanetriyl ester | 38 |
| 63 | 33.7398 | 3.7169 | Dodecanoic acid, 1,2,3-propanetriyl ester | 43 |
| 64 | 33.8584 | 2.5829 | Fumaric acid, 3,5-dichlorophenyl isohexyl ester | 46 |
| 65 | 35.1487 | 0.1552 | Acetamide, N-[2-[[2-[2-(2-nitrophenyl)ethenyl]phenyl]azo]phenyl]- | 91 |

## LIST OF PLATES Appendix B

### Optimization of In situ Transesterification from Orange Peel

| Run | Catalyst wt. (%) | M : O | Temperature (˚C) | Time (min) | Yeild(%) |
|---|---|---|---|---|---|
| 1 | 2.75 | 7.50 | 85.00 | 100.00 | 35.50 |
| 2 | 2.75 | 7.50 | 85.00 | 100.00 | 33.40 |
| 3 | 2.75 | 7.50 | 85.00 | 220.00 | 32.60 |
| 4 | 0.50 | 12.00 | 50.00 | 160.00 | 53.97 |
| 5 | 5.00 | 12.00 | 50.00 | 160.00 | 34.97 |
| 6 | 0.50 | 12.00 | 120.00 | 160.00 | 51.60 |
| 7 | 2.75 | 7.50 | 85.00 | 100.00 | 30.17 |
| 8 | 0.50 | 3.00 | 120.00 | 160.00 | 20.90 |
| 9 | 5.00 | 12.00 | 120.00 | 40.00 | 18.57 |
| 10 | -1.75 | 7.50 | 85.00 | 100.00 | 24.90 |
| 11 | 2.75 | 7.50 | 85.00 | 100.00 | 38.30 |
| 12 | 2.75 | -1.50 | 85.00 | 100.00 | 45.20 |
| 13 | 2.75 | 7.50 | 155.00 | 100.00 | 27.87 |
| 14 | 5.00 | 3.00 | 120.00 | 40.00 | 53.07 |
| 15 | 7.25 | 7.50 | 85.00 | 100.00 | 20.40 |
| 16 | 5.00 | 3.00 | 50.00 | 160.00 | 24.20 |
| 17 | 5.00 | 3.00 | 120.00 | 160.00 | 21.80 |
| 18 | 2.75 | 7.50 | 15.00 | 100.00 | 22.50 |
| 19 | 0.50 | 12.00 | 120.00 | 40.00 | 27.40 |
| 20 | 2.75 | 7.50 | 85.00 | -20.00 | 19.00 |
| 21 | 0.50 | 3.00 | 50.00 | 160.00 | 33.27 |
| 22 | 0.50 | 3.00 | 50.00 | 40.00 | 41.10 |
| 23 | 5.00 | 12.00 | 50.00 | 40.00 | 33.27 |
| 24 | 2.75 | 7.50 | 85.00 | 100.00 | 18.70 |
| 25 | 0.50 | 12.00 | 50.00 | 40.00 | 23.47 |
| 26 | 5.00 | 3.00 | 50.00 | 40.00 | 14.30 |
| 27 | 5.00 | 12.00 | 120.00 | 160.00 | 19.96 |
| 28 | 0.50 | 3.00 | 120.00 | 40.00 | 38.00 |
| 29 | 2.75 | 16.50 | 85.00 | 100.00 | 70.10 |
| 30 | 2.75 | 7.50 | 85.00 | 100.00 | 19.96 |

**Limestone and CaO**
**TGA**

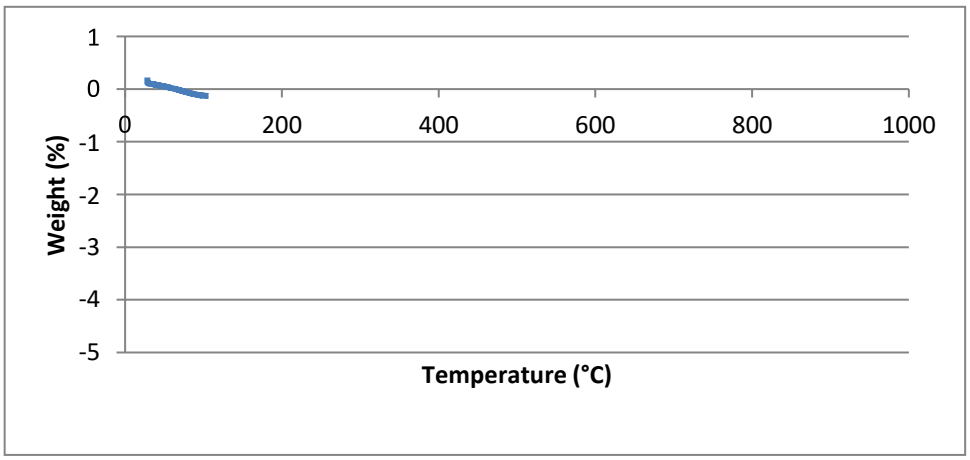


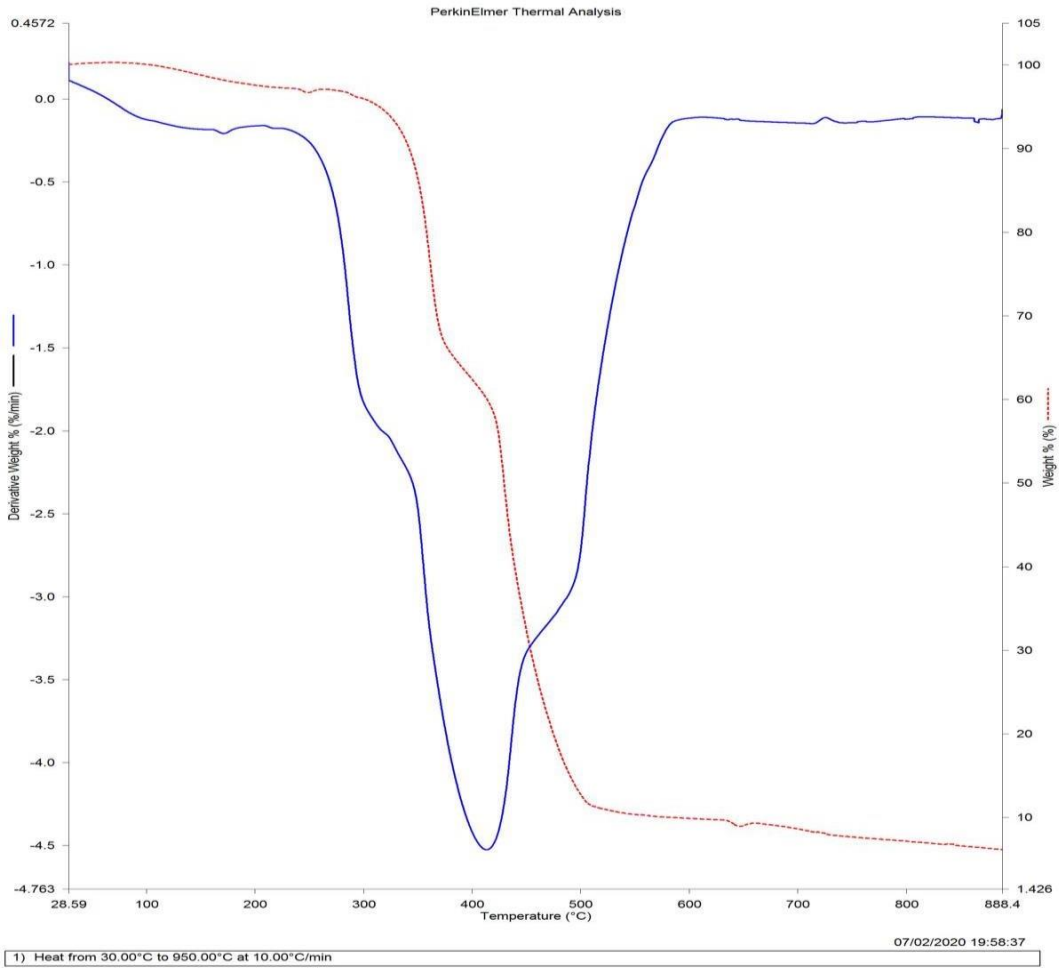

## DA Plot

Data Reduction Parameters

| | | | | | | | |
|---|---|---|---|---|---|---|---|
| | Po override: | 760.00 Torr | | | | | |
| DA Method | Incr. E: | 500.000 | Incr. n: | 0.100 | Interact. Const. (K): | 2.960nm³ x kJ / mol | |
| Adsorbate | Nitrogen | | Temperature | 77.350K | | | |
| | Molec. Wt.: | 28.013 | Cross Section: | 16.200 Å² | Liquid Density: | 0.808 g/cc | |

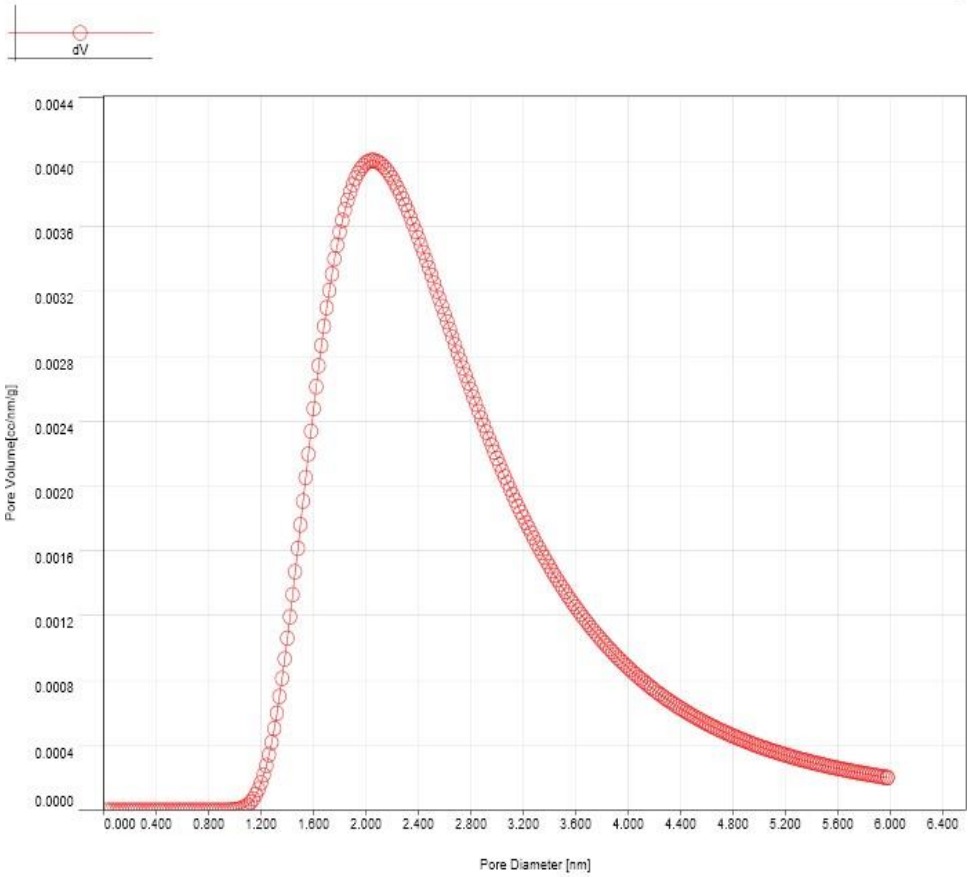


DA method summary

| | |
|---|---|
| Best E = | 2.059 kJ/mol |
| Best n = | 1.000 |
| DA Micropore Volume = | 0.008 cc/g |
| Pore Diameter (mode)= | 2.060e+00 nm |

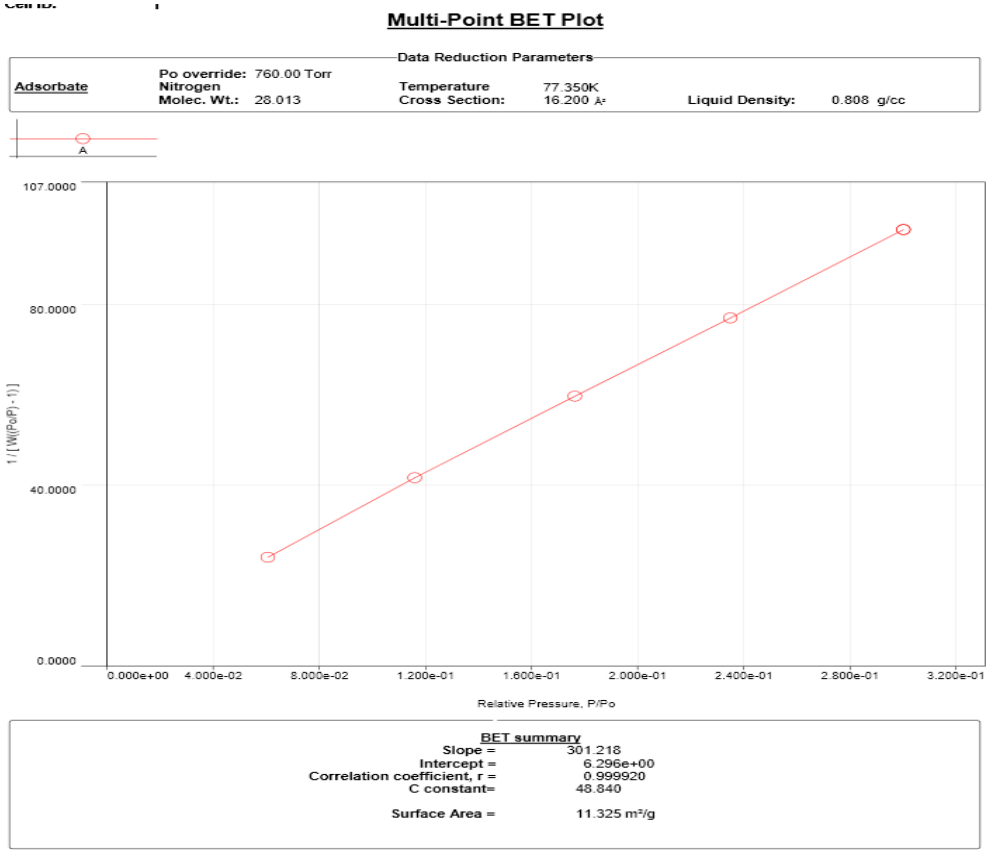


BET Plot for CaO

## DA Plot

**Data Reduction Parameters**

| | | | | | |
|---|---|---|---|---|---|
| DA Method | Po override: | 760.00 Torr | | | |
| Adsorbate | Incr. E: | 500.000 | Incr. n: | 0.100 | Interact. Const. (K): 2.960nm³ x kJ / mol |
| | Nitrogen | | Temperature | 77.350K | |
| | Molec. Wt.: | 28.013 | Cross Section: | 16.200 Å² | Liquid Density: 0.808 g/cc |

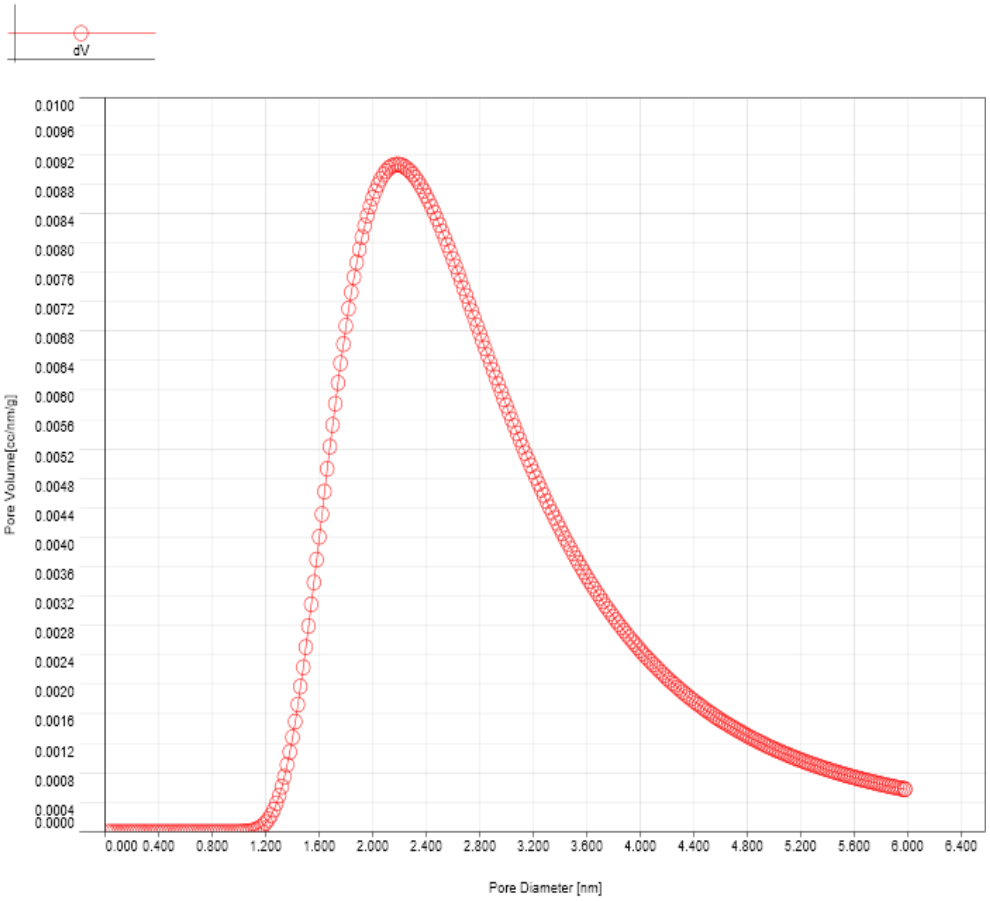


**DA method summary**

| | |
|---|---|
| Best E = | 1.701 kJ/mol |
| Best n = | 1.000 |
| DA Micropore Volume = | 0.019 cc/g |
| Pore Diameter (mode)= | 2.180e+00 nm |

# ABBREVIATIONS

Cell ID: 1

## Multi-Point BET Plot

Data Reduction Parameters

| Adsorbate | Po override: 760.00 Torr | | | | |
|---|---|---|---|---|---|
| | Nitrogen | Temperature | 77.350K | | |
| | Molec. Wt.: 28.013 | Cross Section: | 16.200 Å² | Liquid Density: | 0.808 g/cc |

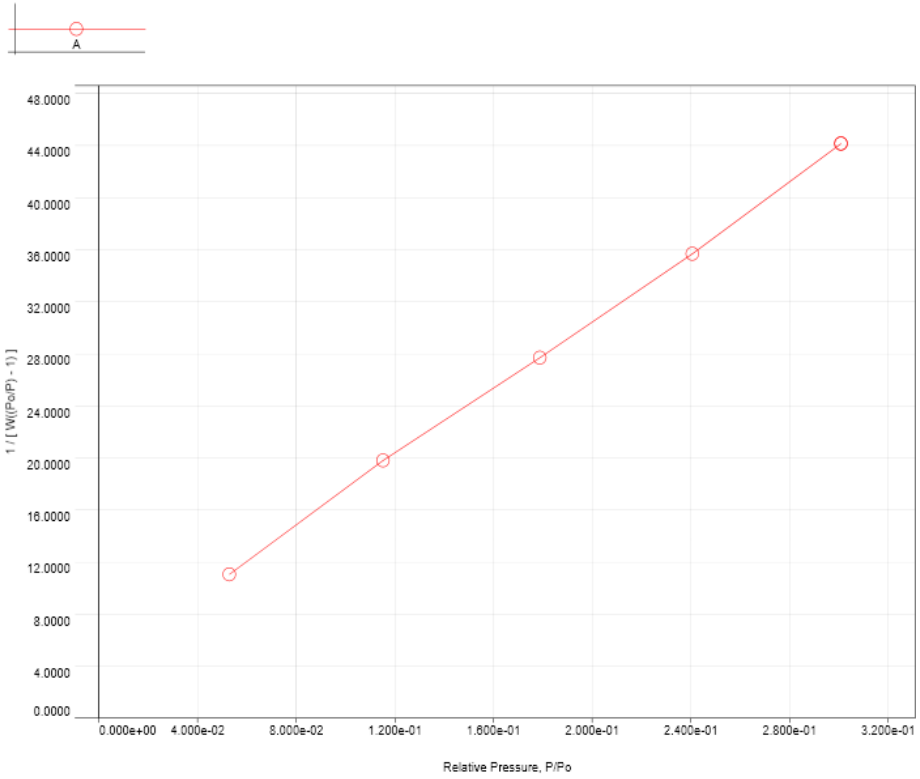


BET summary

| | |
|---|---|
| Slope = | 132.165 |
| Intercept = | 4.194e+00 |
| Correlation coefficient, r = | 0.999776 |
| C constant= | 32.510 |
| Surface Area = | 25.539 m²/g |